CHAPTER 7

Discrete Fourier Transforms

We have already discovered a rich theory of frequency transforms for analog signals, and this chapter extends the theory to discrete signals. In fact, the discrete world presents fewer mathematical subtleties. Several reasons compel us to cover the difficult theory first. It was historically prior, for one thing. Fourier developed his techniques for the practical solution of the heat equation long before engineers worried about pen-and-pencil computations for the frequency content of a sampled signal. Beginning with the treatment of analog frequency transforms furnishes—especially in the case of the classic Fourier series—a very clear foundation for comprehending the idea of the frequency content of a signal. A general periodic signal becomes a sum of familiar sinusoids, each with its well-known frequency value. Finally, it is easy to relate the discrete theory to analog notions and thereby justify the claims that such and such a value does represent the discrete signal spectral content at some frequency.

We begin frequency transforms for discrete signals by covering the discrete Fourier transform (DFT), which Chapters 2 and 4 have already introduced. Chapter 2 covered the DFT only very briefly, in the context of providing an example of an orthonormal subset of the discrete Hilbert space l^2. In studying the analysis of signal textures in Chapter 4, our statistical methods proved inadequate for characterizing certain periodic trends within signals. An example is separating the fine-scale roughness from the coarse-scale waviness of a signal. Although statistical techniques tend to obscure the repetitive appearance of signal features, there is no such problem with spectral texture measures. We found that the magnitude of the inner product of a discrete signal with an exponential provided a translation invariant measure of the presence of a discrete frequency component. Thus, two very different motivations already exist for our pursuit of discrete frequency theory, and the DFT in particular: The complex exponentials upon which it is based are orthogonal on finite intervals $[0, N-1] \subset \mathbb{Z}$, and it is very useful for signal texture analysis.

The discrete world's DFT is analogous to the analog Fourier series. It works with discrete periodic signals. The discovery of a fast algorithm for computing the DFT, called the fast Fourier transform (FFT), coincided with the phenomenal development of computing technology in the middle part of the twentieth century. The

Signal Analysis: Time, Frequency, Scale, and Structure, by Ronald L. Allen and Duncan W. Mills
ISBN: 0-471-23441-9

FFT completely changed the nature of the signal processing discipline and the work habits—indeed the consciousness—of signal analysts [1]. By reducing the complexity of the computation from an $O(N^2)$ algorithm to an $O(N\log_2 N)$ problem, the FFT makes real-time frequency analysis of signals practical on digital computers.

Another discrete transform must be used when studying the frequencies within discrete aperiodic signals. It has a terrible name: the discrete-time Fourier transform (DTFT). Like the DFT, it extracts the frequency content of discrete signals. But unlike the DFT, the DTFT outputs a continuous range of frequencies from an aperiodic input signal. So similar are the acronyms that it is easily confused with the DFT, and, while its appellation boasts "discrete time," this is only a half-truth, because it in fact produces an analog result. Nevertheless, the awful moniker has stuck. We live with it. We repeat it. The DTFT is the discrete world's mirror image of the Fourier transform.

The next chapter covers a generalization of the DTFT, called the z-transform. It has applications in the stability analysis of discrete systems, solutions for discrete-time difference equations, and subsampling and upsampling operations.

This chapter's last sections develop the principles underlying the famous sampling theorem of Shannon[1] and Nyquist.[2] This result effectively builds a frequency analysis bridge between the world of analog signals and the world of discrete signals [2, 3].

7.1 DISCRETE FOURIER TRANSFORM

We have already made acquaintance with the discrete Fourier transform in Chapters 2 and 4. Now we seek a more formal foundation for the theory of the frequency content of discrete signals. All signal frequency analysis applications that rely on digital computers use the DFT, so we will have regular opportunities to refer back to this groundwork and even extend it in the later chapters of this book.

We first took note of the DFT in Chapter 2. The discrete complex exponentials, restricted to a finite interval, are an orthogonal set within the space of square-summable signals, l^2. Thus, if we consider the subspace of l^2 consisting of signals that are zero outside $[0, N-1]$, then the signals

$$u_k(n) = e^{\frac{-j2\pi kn}{N}} [u(n) - u(n-N)], \tag{7.1}$$

[1]Claude E. Shannon (1916–2001) first detailed the affinity between Boolean logic and electrical circuits in his 1937 Master's thesis at the Massachusetts Institute of Technology. Later, at Bell Laboratories, he developed much of theory of reliable communication, of which the sampling theorem is a cornerstone.

[2]Harry Nyquist (1887–1976) left Sweden at age 18 for the United States. As a Bell Laboratories scientist, he provided a mathematical explanation for thermal noise in an electrical resistance, discovered the relation between analog signal frequency and digital sampling rate that now bears his name, and acquired 138 patents.

form an orthogonal set on $[0, N-1]$. We can normalize the family $\{u_k(n) \mid k = 0, 1, 2, ..., N-1\}$ by dividing each signal in (7.1) by $N^{1/2}$. We don't need to consider $k > N-1$, because these signals repeat themselves; this is due to the 2π-periodicity of the exponentials: $\exp(-j2\pi kn/N) = \exp[-j2\pi(k+N)/N]$.

Chapter 4 further acquainted us to the discrete Fourier transform through our study of signal texture. In particular, signals may have different periodic components within them: short-term variations, called roughness (in the parlance of surface metrology), and the long-term variations, called waviness. One way to distinguish and measure the two degrees of repetitiveness is to take the inner product over $[0, N-1]$ of $x(n)$ with exponentials of the form (7.1). Any relatively large magnitude of the resulting inner product, $\langle x(n), \exp(2\pi nk/N)\rangle$ on $[0, N-1]$ indicates a correspondingly large presence of a periodic component of discrete frequency $\omega = 2\pi k/N$. This idea could be augmented by performing a normalized cross-correlation of $x(n)$ with prototype signals $\exp(2\pi nk/N)$ as in Section 4.6.1.

7.1.1 Introduction

Our interest in the discrete Fourier transform is twofold. From the viewpoint of Hilbert spaces—where it furnishes a particularly elegant example of an orthogonal basis—we have a theoretical interest in exploring the discrete Fourier transform. From texture interpretation—the rich, seemingly endless field from which so many research endeavors arise—we acquire a practical interest in better understanding and applying the DFT. Let us then formally define the DFT, prove that it forms a complete representation of discrete periodic signals, and consider some examples.

Definition (Discrete Fourier Transform). Suppose $x(n)$ is a discrete signal and $N > 0$. Then the discrete signal $X(k)$ defined by

$$X(k) = \sum_{n=0}^{N-1} x(n) \exp\left(\frac{-2\pi jnk}{N}\right), \tag{7.2}$$

where $0 \le k \le N-1$, is the *discrete Fourier transform* of $x(n)$ on the interval $[0, N-1]$. Equation (7.2) is called the *analysis equation* for the DFT. In general, $X(k)$ is complex; the complex norm, $|X(k)|$, and complex phase, $\arg(X(k))$, for $0 \le k < N$, are called the *discrete magnitude spectrum* and *discrete phase spectrum,* respectively, of $x(n)$.

DFT conventions vary widely. A popular notation is to use lowercase Latin letters for the time-domain discrete signal, $s(n)$, and the corresponding uppercase letter for the DFT, $S(k)$. Some authors like to use the hat mark: The DFT of $x(n)$ is $X(k)$ Also, the systems theory notation, $S = \mathcal{F}s$, is handy; $\mathcal{F}$ is the discrete system that accepts a signal $s(n)$ with period N and produces its DFT, $S(k)$. Note that the definition of the system $\mathcal{F}$ in this case depends on N. Different values for the period of the discrete input signals produce different discrete systems. We must register yet another warning about the varieties of DFT definitions in the literature. Equation

(7.2) is the most common definition of the DFT in the engineering research literature. There is also a discrete Fourier series (DFS) which multiplies each $X(k)$ in (7.2) by N^{-1}. We introduce the DFS in Section 7.1.2, and there it becomes clear that its particular formulation helps draw a link between analog and discrete frequency transforms. Scientists often define the DFT with a positive exponent. Some authors prefer to normalize the DFT coefficients by a factor of $N^{-1/2}$. Finally, when using mathematical software packages, one must always be alert to the possibility that the package indexes arrays beginning with one, not zero. In such a situation the DC term of the DFT is associated with $k = 1$, the smallest periodic component with $k = 2$ and $k = N$, and so on.

Example (Discrete Delta Signal). Consider the signal $x(n) = [\underline{1}, 0, 0, 0, 0, 0, 0, 0]$ on the interval $[0, 7]$. We have $X(k) = 1$, for $0 \leq k < 8$. So the computation of the delta signal's transform is quite uncomplicated, unlike the case of the analog Fourier series.

Example (Discrete Square Pulse). Consider the signal $x(n) = [1, \underline{1}, 1, 1, 0, 0, 0, 0]$. Its DFT is $X(k) = [\underline{4}, 1–(1 + \sqrt{2})j, 0, 1 – (\sqrt{2} – 1)j, 0, 1 + (\sqrt{2} – 1)j, 0, 1 + (1 + \sqrt{2})j]$. Note the symmetry: $X(k)$ and $X(8 – k)$ are complex conjugates for $0 < k \leq 7$. If we shift the square pulse so that $y(n) = [\underline{0}, 0, 1, 1, 1, 1, 0, 0]$, then $Y(k) = [\underline{4}, –(1 + \sqrt{2})–j, 0, (\sqrt{2} – 1) + j, 0, (\sqrt{2} – 1) – j, 0, –(1 + \sqrt{2}) + j]$. Although the time-domain pulse has translated, the zeros of the frequency-domain coefficients are in the same locations for both $X(k)$ and $Y(k)$. Indeed, there is a time shift property for the DFT, just as we found for the analog Fourier transform and Fourier series. Since $x(n) = y(n – m)$, where $m = 2$, we have $X(k) = Y(k)\exp(–2\pi jkm/8)$. The DFT can be visualized by plotting the coefficients as points in the complex plane, or as separate plots of the magnitude and the phase (Figure 7.1). Since the magnitude of the DFT coefficients do not change with translation of the time-domain signal, it is most convenient to plot the magnitude or the energy components of $X(k)$—$|X(k)|$ or $|X(k)|^2$, respectively.

Example (Ramp Pulse). Consider the signal $x(n) = [\underline{1}, 2, 3, 0, 0, 0]$ on $[0, 5]$, with period $N = 6$. We find $X(k) = 1 + 2\exp(–\pi jk/3) + 3\exp(–\pi jk)$.

7.1.1.1 Inversion Formula.

There is an inversion theorem for the DFT, and, as we found in studying analog transforms, it is the key to understanding the basic properties.

Theorem (DFT Inverse). Suppose $x(n)$ is a discrete signal and $X(k)$ is the DFT of $x(n)$ on $[0, N – 1]$. Then

$$x(n) = \frac{1}{N} \sum_{k=0}^{N-1} X(k) \exp\left(\frac{2\pi jnk}{N} \right). \tag{7.3}$$

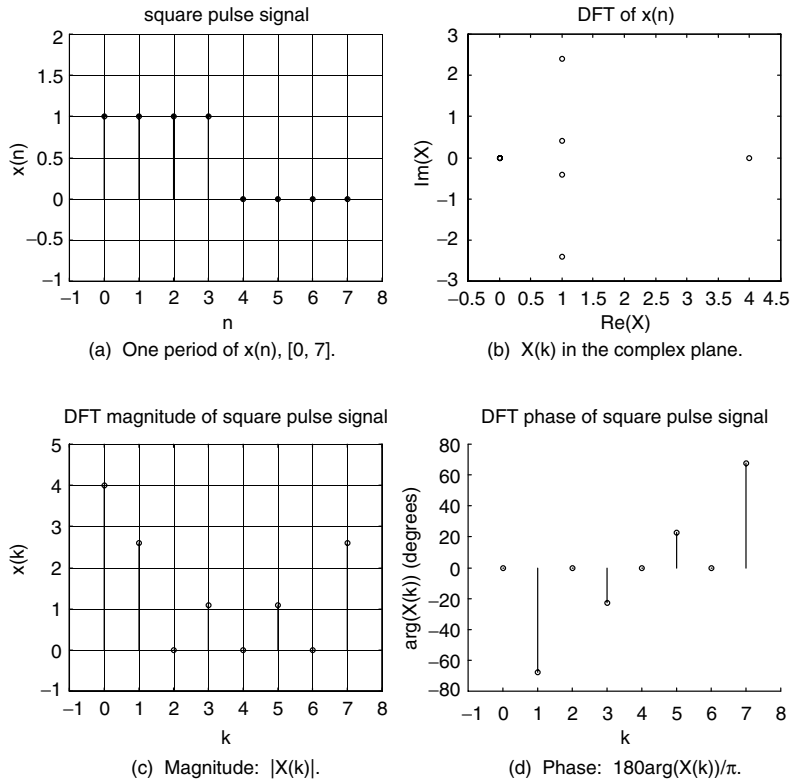

Fig. 7.1. Some examples of the DFT computation. Panel (a) shows a single period of a simple square wave, $x(n)$. In panel (b), the DFT of $x(n)$, $X(k)$ is shown; note that there are only six distinct values, so the circled point at the origin represents three values: $X(2) = X(4) = X(6) = 0$. More revealing is the magnitude of the DFT, $|X(k)|$, shown in panel (c). The phase of $X(k)$ is shown in panel (d); note the linear progression of the phases of the nonzero $X(k)$ values. This clue indicates that DFT coefficients may be visualized as magnitudes associated with points on the unit circle of the complex plane.

Proof: We substitute the expression $X(k)$, given by (7.2) into the right-hand side of (7.3) and work through the exponential function algebra. This brute force attack gives

$$\begin{aligned}\frac{1}{N}\sum_{k=0}^{N-1} X(k)\exp\left(\frac{2\pi jnk}{N}\right) &= \frac{1}{N}\sum_{k=0}^{N-1}\left(\sum_{r=0}^{N-1} x(r)\exp\frac{-2\pi jrk}{N}\right)\exp\left(\frac{2\pi jnk}{N}\right)\\ &= \frac{1}{N}\sum_{r=0}^{N-1}\sum_{k=0}^{N-1} x(r)\exp\left(\frac{-2\pi jrk}{N}\right)\exp\left(\frac{2\pi jnk}{N}\right)\\ &= \sum_{r=0}^{N-1} x(r)\left[\frac{1}{N}\sum_{k=0}^{N-1}\exp\left(\frac{2\pi j(n-r)k}{N}\right)\right], \end{aligned} \tag{7.4}$$

and it appears that we have quite a mess on our hands! However, the following lemma shows that the bracketed expression in (7.4) has a gratifying, simple form.

Lemma. Let $N > 0$, and let p and k be integers. Then, if for some $m \in \mathbb{Z}$, we have $p = mN$, then

$$\frac{1}{N}\sum_{k=0}^{N-1} \exp\left(\frac{2\pi jpk}{N}\right) = 1; \tag{7.5a}$$

otherwise

$$\frac{1}{N}\sum_{k=0}^{N-1} \exp\left(\frac{2\pi jpk}{N}\right) = 0. \tag{7.5b}$$

Proof of lemma: Let $a = \exp(2\pi jp/N)$. Then, expanding the summation, for instance in (7.5a), gives

$$\frac{1}{N}\sum_{k=0}^{N-1} \exp\left(\frac{2\pi jpk}{N}\right) = \frac{1}{N}\left(1 + a + a^2 + \cdots + a^{N-1}\right). \tag{7.6}$$

But if $p = mN$, then $a = \exp(2\pi jmN/N) = \exp(2\pi jm) = 1$. In this case, the right-hand side of (7.6) is unity. If $p/N \notin \mathbb{Z}$, then $a \neq 1$ and $1 - a \neq 0$. This implies $1 + a + a^2 + \cdots + a^{N-1} = (1 - a^N)/(1 - \mathrm{a})$. However, $aN = 0$, and in this case the right-hand side of (7.6) is zero, proving the lemma. ■

Let us then continue proving the theorem. The term $(n - r)$ in the bracketed expression in (7.4) is either an integral multiple of N or it is not. Suppose $p = (n - r) = mN$ for some $m \in \mathbb{Z}$; by the lemma, therefore, the bracketed expression is unity. But since $0 \leq n, r \leq N - 1$, we know that $p = n - r$ is a multiple of N only if $n - r = 0$, that is, $n = r$. So the bracketed sum in (7.4) is zero unless $n = r$:

$$\frac{1}{N}\sum_{k=0}^{N-1} \exp\left(\frac{2\pi j(n-r)k}{N}\right) = \begin{cases} 0 & n \neq r, \\ 1 & \text{otherwise.} \end{cases} \tag{7.7}$$

Thus, the whole expression in (7.4) reduces to $x(n)$, and the proof of the theorem is complete. ■

Definition (Inverse DFT). Equation (7.3) is called the *synthesis equation* for the DFT. The expression (7.3) is also called the inverse discrete Fourier transform (IDFT).

The first term, $X(0)$, is often called the DC (direct current) component of the DFT for $x(n)$, since it contains no periodic (i.e., alternating current) component. This whispers of Fourier analysis's electrical engineering heritage, although

nowadays everyone—engineers, scientists, even university business school professors running trend analyses—uses the term. Note that when $x(n)$ is reconstructed from its DFT, the synthesis equation summation begins with the factor $X(0)/N$, which is the average value of $x(n)$ on the interval $[0, N-1]$.

Corollary (Discrete Fourier Basis). Let K be the set of discrete signals supported on the interval $[0, N-1]$, and let $u(n)$ be the unit step signal. Then K is a Hilbert subspace of l^2, and the windowed exponential signals, $\{u_k(n) \mid 0 \le k \le N-1\}$, where

$$u_k(n) = \frac{\exp(2\pi jkn/N)}{\sqrt{N}}[u(n) - u(n-N)], \tag{7.8}$$

form an orthonormal basis for K.

Proof: Recall from Section 2.7.1 that a Hilbert subspace is an inner product subspace that is complete in the sense that every Cauchy sequence of elements converges to a subspace element. This is easy to show for K. So let us consider the windowed exponentials (7.8). Note that if $0 \le k, \mathrm{l} \le N-1$, then

$$\langle u_k, u_l \rangle = \sum_{n=0}^{N-1} \frac{\exp(j2\pi kn/N)}{\sqrt{N}} \overline{\frac{\exp(j2\pi ln/N)}{\sqrt{N}}} = \frac{1}{N} \sum_{n=0}^{N-1} \exp[j2\pi(k-l)n/N]. \tag{7.9}$$

The theorem's lemma shows that the sum on the right-hand side of (7.9) is zero unless $k = \mathrm{l}$, in which case it is unity. But this is precisely the orthonormality condition. We must show too that the orthonormal set is complete; that is, we need to show the other sense of completeness, which specifies that every element of the subspace K is arbitrarily close to a linear combination of elements of $\{u_k(n) \mid 0 \le k \le N-1\}$. Let $X(k)$ be given by (7.2). For $0 \le n \le N-1$, the theorem implies

$$x(n) = \frac{1}{N} \sum_{k=0}^{N-1} X(k) \exp\left(\frac{2\pi jnk}{N}\right) = \frac{1}{\sqrt{N}} \sum_{k=0}^{N-1} X(k) u_k(n). \tag{7.10}$$

This shows that $x(n)$ is a linear combination of the $\{u_k(n)\}$. ■

Corollary (DFT for Discrete Periodic Signals). Suppose $x(n)$ is a discrete signal with period $N > 0$: $x(n) = x(n+N)$ for all n. Then,

$$x(n) = \frac{1}{N} \sum_{k=0}^{N-1} X(k) \exp\left(\frac{2\pi jnk}{N}\right). \tag{7.11}$$

for all n.

Proof: Note that on the finite interval $[0, N-1]$, the theorem implies (7.11). But $x(n) = x(n+N)$, and the right-hand side of (7.11) is also periodic with period N, so the corollary holds. ■

Corollary (DFT Uniqueness). Suppose $x(n)$ and $y(n)$ are discrete signals, and $X(k)$ and $Y(k)$ are their respective DFTs on $[0, N-1]$. If $X = Y$ on $[0, N-1]$, then $x(n) = y(n)$ on $[0, N-1]$.

Proof: If $X(k) = Y(k)$ for all $0 \le k \le N-1$, then both $x(n)$ and $y(n)$ are given by the same inversion formula (7.3). So $x(n) = y(n)$ for all $0 \le n \le N-1$. ■

So the transform's uniqueness on an interval follows from the inversion equation. We followed a similar roundabout route toward showing transform uniqueness with the analog Fourier series and Fourier transform. In the analog world, the integration of signals, possibly containing discontinuities, complicates the uniqueness propositions, of course. Supposing Riemann integration, we can claim uniqueness only up to a finite number of impulse discontinuities. And, allowing the more robust Lebesgue integration, we can only claim that signals that are equal, except perhaps on a set of measure zero, have identical transforms. However, with discrete signals, owing to the finite sums used in computing the DFT, the transform values are truly unique.

Corollary (DFT Uniqueness). Suppose $x(n)$ and $y(n)$ discrete signals, both with period equal to N. If their DFTs are equal, $X(k) = Y(k)$ for all $0 \le k \le N-1$, then $x(n) = y(n)$ for all n.

Proof: Combine the proofs of the previous two corollaries. ■

If $X(k) = Y(k)$ for all $0 \le k \le N-1$, then both $x(n)$ and $y(n)$ are given by the same inversion formula (7.3). So $x(n) = y(n)$ for all $0 \le n \le N-1$.

The DFT Uniqueness Corollary encourages us to characterize the DFT as the appropriate transform for periodic discrete signals. If a signal $x(n)$ has period $N > 0$, then, indeed, the synthesis equation provides a complete breakdown of $x(n)$ in terms of a finite number of exponential components. But, the DFT is also applied to the restriction of aperiodic discrete signals to an interval, say $s(n)$ on $[a, b]$, with $b - a = N - 1$. In this case, the analysis equation (7.2) is used with $x(n) = s(a-n)$. Of course, the synthesis equation does not give $s(n)$; rather, it produces the periodic extension of $s(n)$ on $[a, b]$.

7.1.1.2 Further Examples and Some Useful Visualization Techniques.

Therefore, let us explore a few examples of the DFT's analysis and synthesis equations before proceeding to link the DFT to the frequency analysis of analog signals. These examples show that it is quite straightforward to compute the DFT analysis equations coefficients $X(k)$ for a trigonometric signal $x(n)$. It is not necessary, for instance, to explicitly perform the sum of products in the DFT analysis equation (7.2).

Example (Discrete Sinusoids). Consider the discrete sinusoid $x(n) = \cos(\omega n)$. Note that $x(n)$ is periodic if and only if ω is a rational multiple of 2π: $\omega = 2\pi p/q$ for some $p, q \in \mathbb{Z}$. If $p = 1$ and $q = N$, then $\omega = 2\pi/N$, and $x(n)$ is periodic on $[0, N-1]$ with fundamental period N. Signals of the form $\cos(2\pi kn/N)$ are also periodic on $[0, N-1]$, but since $\cos(2\pi kn/N) = \cos(2\pi(N-k)n/N)$, they are different only for $k = 1, 2, ..., \lfloor N/2 \rfloor$. We recall these facts from the first chapter and note that a like result holds for discrete signals $y(n) = \sin(\omega n)$, except that $\sin(2\pi kn/N) = -\sin(2\pi(N-k)n/N)$. We can explicitly write out the DFT synthesis equations for the discrete sinusoids by observing that

$$\cos\left(\frac{2\pi nk}{N}\right) = \frac{1}{2}\exp\left(\frac{2\pi jnk}{N}\right) + \frac{1}{2}\exp\left(\frac{2\pi jn(N-k)}{N}\right), \tag{7.12a}$$

$$\sin\left(\frac{2\pi nk}{N}\right) = \frac{1}{2j}\exp\left(\frac{2\pi jnk}{N}\right) - \frac{1}{2j}\exp\left(\frac{2\pi jn(N-k)}{N}\right), \tag{7.12b}$$

for $0 \le k \le \lfloor N/2 \rfloor$. Equations (7.12a) and (7.12b) thereby imply that $X(k) = X(N-k) = N/2$ with $X(m) = 0$, for $0 \le m \le N-1$, $m \ne k$; and $Y(k) = -Y(N-k) = (-jN/2)$, with $Y(m) = 0$, for $0 \le m \le N-1$, $m \ne k$. The factor of N in the expressions for $X(k)$ and $Y(k)$ ensures that the DFT synthesis equation (7.3) holds for $x(n)$ and $y(n)$, respectively.

Example (Linear Combinations of Discrete Sinusoids). If we multiply a discrete sinusoid by a constant scale factor, $v(n) = Ax(n) = A\cos(\omega n)$, then the DFT coefficients for $v(n)$ are $V(k) = AX(k)$. This is a *scaling* property of the DFT. This is clear from the analysis (7.2) and synthesis (7.3) equations. Furthermore, if $v(n) = x(n) + y(n)$, then $V(k) = X(k) + Y(k)$, where $V(k)$, $X(k)$, and $Y(k)$ are the DFT coefficients of $v(n)$, $x(n)$, and $y(n)$, respectively. This is a *superposition* property of the DFT. Thus, it is easy to find the DFT synthesis equation for a linear combinations of discrete sinusoids from this linearity property and the previous example.

Example (Phase of Discrete Sinusoids). If the sinusoid $x(n) = \cos(\omega n)$ has period $N > 0$, then so does $y(n) = \cos(\omega n + \phi)$. Since $y(n) = [\exp(j\omega n + j\phi) + \exp(-j\omega n - j\phi)]/2 = [\exp(j\phi)\exp(j\omega n) + \exp(-j\phi)\exp(-j\omega n)]/2$, we can use the scaling and superposition properties of the previous example to find the DFT coefficients of $Y(k)$ in terms of $X(k)$. Notice also that the sinusoidal signal's phase shift, ϕ, does not change the complex magnitude of the DFT coefficients. This property we noted in our study of textured signal periodicity in Chapter 4.

A common and useful notation allows us to write the DFT is a more compact form.

Definition (Phase Factor). For $N > 0$, the Nth root of unity, $W_N = e^{-2\pi j/N}$, is called the *phase factor* of order N.

The fast Fourier transform algorithms in Section 7.1.4 exploit the symmetries of the phase factor that appear in the DFT analysis and synthesis equations.

Now, the powers of W_N, $(W_N)^k = e^{-2\pi jk/N}$, $0 \le k < N$, all lie on the unit circle in the complex plane: $(W_N)^k = e^{-2\pi jk/N} = \cos(2\pi k/N) - j\sin(2\pi k/N)$. Then we can rewrite the DFT analysis and synthesis equations as follows:

$$X(k) = \sum_{n=0}^{N-1} x(n) W_N^{nk}, \tag{7.13}$$

$$x(n) = \frac{1}{N} \sum_{k=0}^{N-1} X(k) W_N^{-nk}. \tag{7.14}$$

Thus, $X(k)$ is a polynomial of degree $N-1$ in $(W_N)^k$, and $x(n)$ is a polynomial of degree $N-1$ in $(W_N)^{-n}$. That is, if we define the complex polynomials, $P(z) = x(0) + x(1)z + x(2)z^2 + \cdots + x(N-1)z^{N-1}$ and $p(z) = (1/N)[X(0) + X(1)z + X(2)z^2 + \cdots + X(N-1)z^{N-1}]$, then $X(k) = P((W_N)^k)$, and $x(n) = p((W_N)^{-n})$. The DFT of $x(n)$ is just the complex polynomial $P(z)$ evaluated at specific points on the unit circle, namely $(W_N)^k = e^{-2\pi jk/N}$, $0 \le k < N$. Similarly, the IDFT is the complex polynomial $p(z)$ evaluated at points $(W_N)^{-n}$ on the unit circle, $0 \le n < N$. In fact, these are the same points, just iterated in the opposite order. We will extend this idea of representing the DFT as a complex polynomial restricted to a set of discrete points in the next chapter; in fact, the concept of the z-transform carries it to the extreme. For now we just want to clarify that the DFT coefficients can be thought of as functions of an integer variable k or of points on the unit circle $z = \cos(2\pi k/N) - j\sin(2\pi k/N)$. This idea enables us to better visualize some of the behavior of the transform for specific signals. For example, we may study the transforms of square pulse signals for various periods N and various duty cycles (percent of non zero coefficients) as in Figure 7.2.

For square pulse signals, such as in Figure 7.2, there is a closed-form expression for the DFT coefficients. Suppose $x(n)$ has period $N > 0$, and $x(n)$ is zero except for the first M values, $x(0) = x(1) = \cdots = x(\mathrm{M}-1) = 1$, with $0 < M < N-1$. Then $X(k)$ is a partial geometric series in $(W_N)^k$: $X(k) = 1 + (W_N)^k + (W_N)^{2k} + \cdots + (W_N)^{k(M-1)}$. Assuming that $(W_N)^k \neq 1$, we calculate

$$X(k) = \frac{1 - \left(W_N^k\right)^M}{1 - W_N^k} = \frac{W_N^{kM/2}\left(W_N^{-kM/2} - W_N^{kM/2}\right)}{W_N^{k/2}\left(W_N^{-k/2} - W_N^{k/2}\right)} = \frac{W_N^{kM/2}\left(e^{\pi jkM/N} - e^{-\pi jkM/N}\right)}{W_N^{k/2}\left(e^{\pi jk/N} - e^{-\pi jk/N}\right)}$$

$$= \frac{W_N^{kM/2}\left(2j\sin(\pi kM/N)\right)}{W_N^{k/2}\left(2j\sin(\pi k/N)\right)} = W_N^{k(M-1)/2}\frac{\left(\sin(\pi kM/N)\right)}{\left(\sin(\pi k/N)\right)} \tag{7.15}$$

Thus, for $k = 0$, $X(k) = M$, and for $0 < k < M-1$, the DFT coefficient $X(k)$ is given by the product of a complex $2N$th root of unity and a ratio of sinusoids: $\sin(\pi kM/N)$ and $\sin(\pi k/N)$. Since $\sin(\pi kM/N)$ oscillates M times faster than $\sin(\pi k/N)$, there are

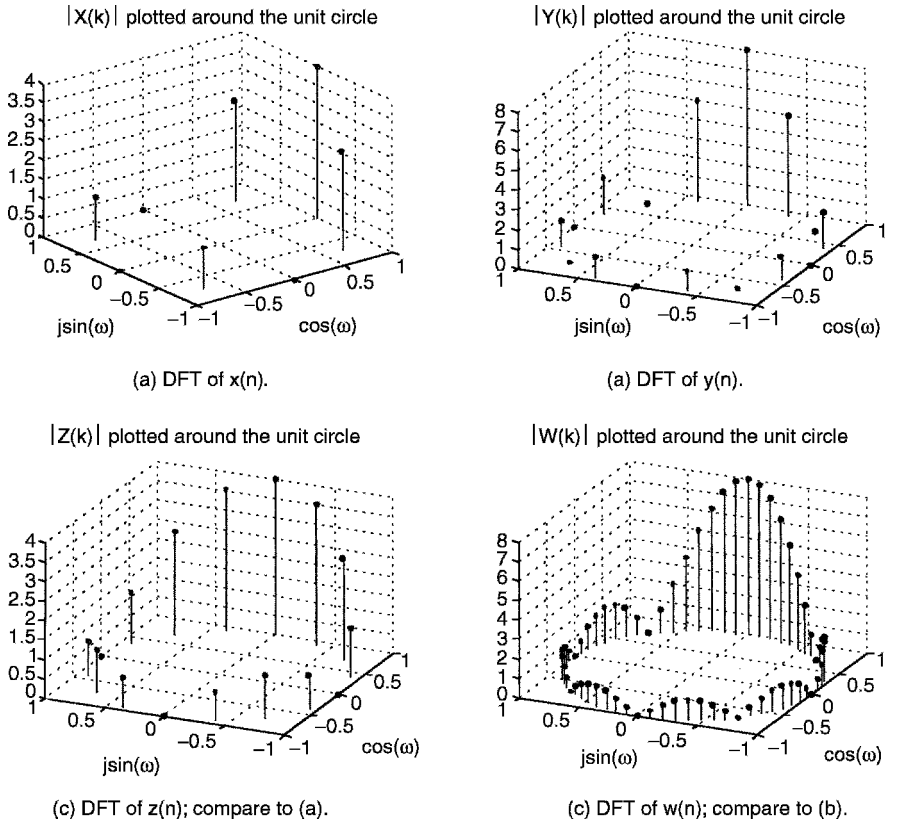

Fig. 7.2. Visualizing the DFT around the unit circle of the complex plane. We set $\omega = 2\pi k/N$ and plot the DFT magnitudes of some signals relative to cos(ω) and sin(ω) around the unit circle in the complex plane. In part (a), $|X(k)|$ for $x(n) = [\underline{1}, 1, 1, 1, 0, 0, 0, 0]$. In part (b), $|Y(k)|$ for $y(n) = [\underline{1}, 1, 1, 1, 1, 1, 1, 1, 0, 0, 0, 0, 0, 0, 0, 0]$. In part (c), $|Z(k)|$ for $z(n) = [\underline{1}, 1, 1, 1, 0, 0, 0, 0, 0, 0, 0, 0, 0, 0, 0, 0]$. In part (d), $w(n)$ has period $N = 64$, with $w(n) = 1$ for $0 \leq n \leq 7$, and $w(n) = 0$ otherwise. Note that the size of the square pulse within the signal's period determines the number of lobes, and the number of analysis equation summands determines the detail within the lobes.

M lobes in the discrete magnitude spectrum $|X(k)|$, if we count the big lobe around $k = 0$ twice (Figure 7.2).

7.1.1.3 Simple Applications. Let us briefly show how to use the DFT in applications on real sampled signal data. This section shows how the magnitudes of DFT coefficients indicate significant periodic trends in the original analog signal. As an example, we perform a discrete Fourier analysis of the solar disturbances associated with sunspots. Most people are aware that sunspot numbers increase dramatically during these solar disturbances, affect high-frequency radio communication on earth, and tend to occur in approximately 11-year cycles.

Since discrete signals arise from sampling analog signals, the first step is to suppose $x(n) = x_a(nT)$, where $x_a(t)$ is an analog signal, $T > 0$ is the sampling interval, and $x_a(t)$ has period NT. If we write $x(n)$ in terms of its DFT synthesis equation (7.3), then we see that the sinusoidal components of smallest frequency are for $k = 1$ and $k = N - 1$: $\cos(2\pi n/N)$, $\sin(2\pi n/N)$, $\cos(2\pi(N-1)n/N)$, and $\sin(2\pi(N-1)n/N)$. These discrete sinusoids come from sampling analog sinusoids with fundamental period NT, for example, $\sin(2\pi n/N) = \sin(2\pi t/(NT))|_{t=Tn}$. But this is precisely the analog sinusoid with fundamental frequency $1/NT$ Hz.

Application (Wolf Sunspot Numbers). The first chapter introduced the Wolf sunspot numbers as an example of a naturally occurring, somewhat irregular, but largely periodic signal. From simple time-domain probing of local signal extrema, we can estimate the period of the sunspots. The DFT is a more powerful tool for such analyses, however. Given the Wolf sunspot numbers over some 300 years, a good estimate of the period of the phenomenon is possible. Figure 7.3 shows the time-domain sunspot data from 1700 to 1996. The sampling interval T is 1 year ($T = 1$), and we declare 1700 to be year zero for Wolf sunspot number data. Thus, we perform a frequency analysis of the signal, using the DFT on $w(n)$ over the interval [1700–1700, 1996–1700] = [0, $N - 1$]. Figure 7.3 shows the DFT, $W(k)$, and its magnitude; there is a huge peak, and for that the rest of the analysis is straightforward. Brute force search finds the maximum magnitude $|W(k)|$ for $0 < k < (1996–1700 + 1)/2$ at time instant $k = k_0$. We do not need to consider higher k values, since the terms above $k = 148 = \lfloor 297/2 \rfloor$ represent discrete frequencies already counted

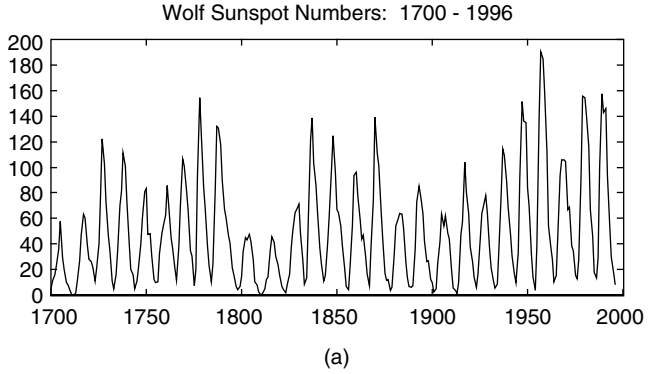

Fig. 7.3. Wolf sunspot numbers. Signal $w(n)$ is the Wolf sunspot number, a composite figure equal to $10G + S$, where G is the average number of sunspot groups and S is the average number of spots reported by a team of international observers. In panel (a), the time-domain plot of $w(n)$ from 1700 to 1996 is shown; note the periodicity. Panel (b) plots the DFT coefficients $W(k)$ in the complex plane but this representation does not aid interpretation. The power of the DFT signal, $P(k) = |W(k)|^2$, appears in panel (c), with the DC term zeroed. The maximum power value occurs at $k = 27$, which represents a sinusoidal component with a period of $297/27 = 11$ years.

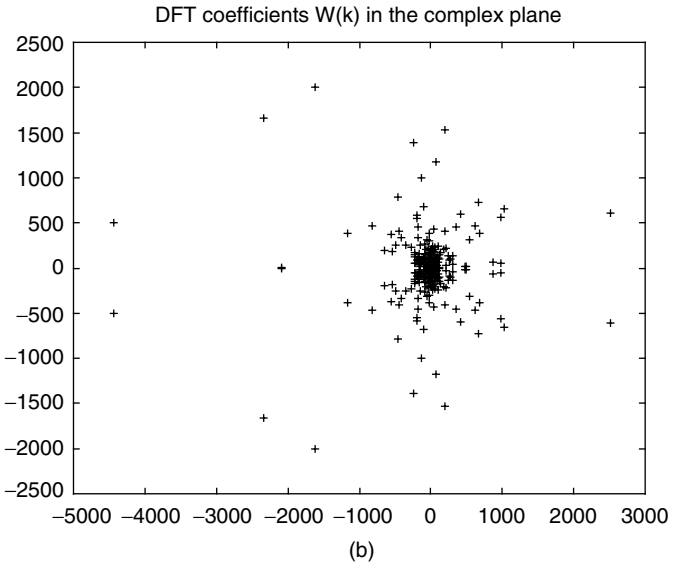

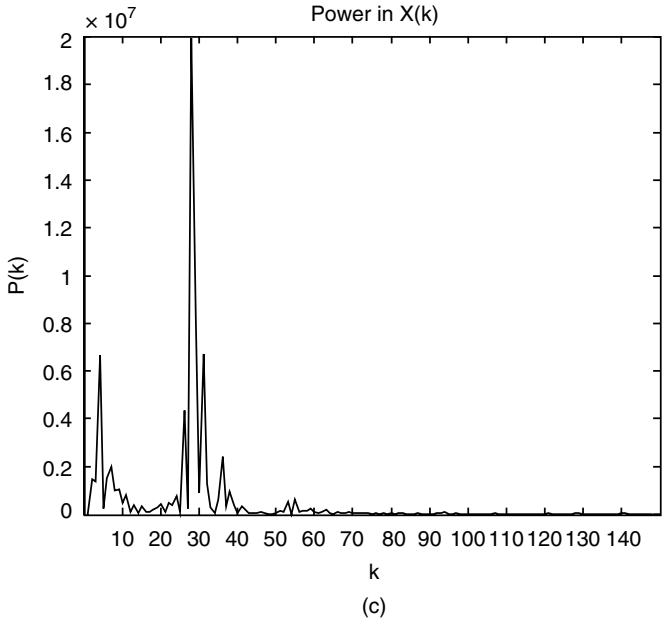

Fig. 7.3 (*Continued*)

among the lower k values. The frequency resolution of the DFT on $N = 297$ samples, each separated by $T = 1$ year, is $1/NT$. Therefore, the biggest periodic component in the sunspot cycle is k_0/NT cycles/year, and this corresponds to a sunspot period of NT/k_0 years.

This same analysis serves other oscillatory signal analysis applications considered already: electrocardiology, manufactured surface waviness analysis, and tone detection. We will consider its further practical uses, strengths, and weaknesses in Chapter 9.

Note that the theoretical presentation of the DFT proceeds in a completely formal manner. A modest amount of algebra, along with the nice properties of the complex exponential signal, are just enough to develop a complete theory. There are no subtleties concerning discontinuities such as we had to overcome with the analog Fourier series. The discrete nature of the signals and the decomposition of a discrete periodic signal into a finite set of discrete exponentials demand no exotic tools such as distributions or Dirac delta functions. The complex exponential signal's elegance and a little algebra are sufficient to develop the entire theory. We could now prove a bunch of theorems about properties of the DFT. But our goal is develop the tools, the understanding, and the fundamental insights of signal analysis; we should not think to just throw the theory at the reader. Before proceeding to a lengthy list of the DFT's properties, let's explore the links that the DFT shares with the tools we already know for the frequency analysis of analog signals. In particular, we shall show that a discrete signal's DFT coefficients approximate certain of the Fourier series coefficients for an analog periodic source signal.

7.1.2 The DFT's Analog Frequency-Domain Roots

Perhaps the clearest insight into how the discrete Fourier transform reveals the frequency content of a discrete signal is to explore its relationship to the Fourier series for analog periodic signals. We begin by defining a variant of the DFT that takes a form very similar to the analog Fourier series.

Definition (Discrete Fourier Series). Suppose $x(n)$ is a discrete signal and $N > 0$. Then the discrete signal $c(k) = c_k$, defined by

$$c(k) = \frac{1}{N} \sum_{n=0}^{N-1} x(n) \exp\left(\frac{-2\pi jnk}{N} \right) \tag{7.16}$$

where $0 \le k \le N - 1$, is the *discrete Fourier series* (DFS) of $x(n)$ on the interval $[0, N - 1]$. Equation (7.16) is called the DFS *analysis equation* for $x(n)$.

Note that if $x(n)$ has DFT coefficients $X(k)$ and DFS coefficients $c(k)$ on $[0, N - 1]$, then $X(k) = c(k)/N$. Except for the factor N, the DFT and the DFS share an

identical theory. Corresponding to the DFT's synthesis equation, there is a DFS *synthesis equation*:

$$x(n) = \sum_{k=0}^{N-1} c(k) \exp\left(\frac{2\pi jnk}{N}\right), \tag{7.17}$$

where $c(k)$ are the DFS analysis equation coefficients for $x(n)$ on $[0, N-1]$. Equation (7.17) also defines the inverse discrete Fourier series (IDFS). The two concepts are so similar that in the literature one must pay close attention to the particular form of the definitions of the DFT and DFS.

The next theorem clarifies the relationship between the DFS and the analog Fourier series. This shows that these discrete transforms are in fact simple approximations to the FS coefficients that we know from analog signal frequency theory. We are indeed justified in claiming that the DFS and DFT provide a frequency-domain description of discrete signals.

Theorem (Relation Between DFS and FS). Let $x_a(t)$ be an analog signal with period $T > 0$. Suppose $N > 0$, $\Delta t = T/N$, $F = 1/T$, and $x(n) = x_a(n\Delta t)$ is a discrete signal that samples $x_a(t)$ at intervals Δt. Finally, let $c(k)$ be the kth DFS coefficient (7.16) for $x(n)$, and let $c_a(k)$ is the kth analog Fourier series coefficient for $x_a(t)$ on $[0, T]$. That is,

$$c_a(k) = \frac{1}{T}\int_0^T x(t)e^{-j2\pi kFt}\,dt, \tag{7.18}$$

where $0 < k < N-1$. Then, $c(k)$ is the trapezoidal rule approximation to the FS integral (7.18) for $c_a(k)$, using the intervals $[0, \Delta t]$, $[\Delta t, 2\Delta t]$, ..., $[(N-1)\Delta t, N\Delta t]$.

Proof: The integrand in (7.18) is complex, but the trapezoidal rule can be applied to both its real and imaginary parts. Suppose we let $y(t) = x_a(t)\exp(-j2\pi kFt)$ be the integrand. Recalling the trapezoidal rule from calculus (Figure 7.4), we can see that a typical trapezoid has a base of width Δt and average height $[y(n\Delta t) + y((n+1)\Delta t)]/2$. In other words, an approximation to $c_a(k)$ is

$$\hat{c}_a(k) = \frac{1}{T}\left\{\begin{array}{c}\left(\dfrac{y(0\cdot\Delta t)+y(1\cdot\Delta t)}{2}\right)\Delta t + \left(\dfrac{y(1\cdot\Delta t)+y(2\cdot\Delta t)}{2}\right)\Delta t + \cdots \\ + \left(\dfrac{y((N-1)\cdot\Delta t)+y(N\cdot\Delta t)}{2}\right)\Delta t\end{array}\right\}. \tag{7.19}$$

Collecting terms inside the braces of (7.18) and observing that $y(0) = y(N\Delta t) = y(T)$ gives

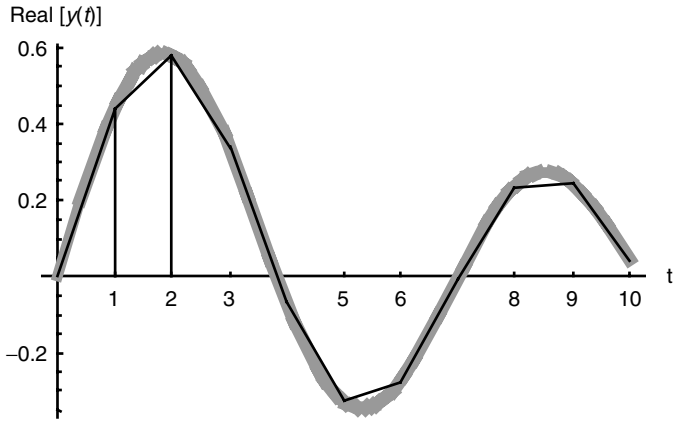

Fig. 7.4. Approximating the Fourier series integral by the trapezoidal rule. The signal $x_a(t)$ has period $T > 0$. The trapezoidal rule applies to the real and imaginary parts of the integrand in the Fourier series analysis equation, $y(t) = x_a(t)\exp(-j2\pi kFt)$. It is necessary to include sufficient trapezoids to span an entire period of the analog signal $x(t)$; in this illustration $T = 10$.

$$\hat{c}_a(k) = \frac{\Delta t}{T}\sum_{n=0}^{N-1} x_a(n\Delta t)\exp(-j2\pi kFn\Delta t) = \frac{1}{N}\sum_{n=0}^{N-1} x(n)\exp\left(\frac{-j2\pi kn}{N}\right) = c(k). \quad (7.20)$$

This shows that the trapezoidal rule approximation to the FS integral is precisely the DFS coefficient $c(k)$ and completes the proof. ■

Thus, the DFS is a straightforward approximation of the analog Fourier series components. And the DFT is just the DFS scaled by the period of the discrete signal. Again, these transforms are appropriate for discrete periodic signals. Of course, one may take any discrete signal, $x(n)$, restrict it to a finite interval, $[0, N-1]$, where $N > 0$, and then perform the DFT analysis equation computation for the $x(n)$ values for $0 \le n < N$. The result is N complex numbers, $X(0), X(1), \ldots, X(N-1)$. This is like computing the DFT for the periodic extension of $x(n)$. The result of computing the IDFT on $X(0), X(1), \ldots, X(N-1)$, is not the original signal $x(n)$; it is $x_p(n) = (1/N)[X(0) + X(1)e^{2\pi jkn/N} + \cdots + X(N-1)e^{2\pi j(N-1)n/N}$, which is periodic with period N. Another transform is necessary for the study of frequency in aperiodic signals—the discrete-time Fourier transform (DTFT). As the DFT is the discrete world's replica of the Fourier series, so the counterpart to Fourier transform for discrete signals is the DTFT. Before considering the aperiodic case, however, let us explain some of the properties of the DFT and how these lead to efficient algorithms for its computation.

7.1.3 Properties

This section explains the many elegant properties of the discrete Fourier transform. Generally speaking, these theorems on linearity, symmetry, and conservation of signal

energy result from the special algebraic characteristics of the complex exponential function. Interesting in themselves, they are useful as well in analyzing signals. As an example, the energy in DFT coefficients does not change as the underlying periodic signal is translated. This property we noted in Chapter 4, and its motivation was our search for a translation-invariant, spatial-frequency-based texture indicator. Our further studies of the properties of DFT, especially its computational symmetries, will lead to the fast Fourier transform (FFT) algorithm. For signals with certain periods—especially powers of two—the FFT offers a dramatic reduction in the computational burden of computing discrete frequency components with the DFT.

Let us begin with some basic properties of the DFT. We have already noted that the DFT of a signal $x(n)$ on $[0, N-1]$, $N > 0$, has period N.

Proposition (Linearity, Time Shift, and Frequency Shift). Let $x(n)$ and $y(n)$ be periodic signals with period $N > 0$, let a and b be constants, and let $X(k)$ and $Y(k)$ be their DFTs, respectively. Then:

(a) (Linearity) The DFT of $ax(n) + by(n)$ is $aX(k) + bY(k)$.
(b) (Time Shift) The DFT of $x(n-m)$ is $(W_N)^{km}X(k)$.
(c) (Frequency Shift) The IDFT of $X(k-m)$ is $(W_N)^{-nm}x(n)$.

In other words, delaying a time-domain signal by m samples is equivalent to multiplying each DFT coefficient in the frequency domain, $X(k)$, by the factor $(W_N)^{km} = e^{-2\pi jkm/N}$. And delaying the frequency-domain signal $X(k)$ by m samples reflects a time-domain multiplication of each value $x(n)$ by $(W_N)^{-nm}$.

Proof: Linearity is easy and left as an exercise. Let $z(n) = x(n-m)$ and let $r = n-m$. Let's apply the DFT analysis equation directly to $z(n)$:

$$\begin{aligned} Z(k) &= \sum_{n=0}^{N-1} z(n)\exp\left(\frac{-j2\pi kn}{N}\right) = \exp\left(\frac{-j2\pi km}{N}\right)\sum_{n=0}^{N-1} x(n-m)\exp\left(\frac{-j2\pi k(n-m)}{N}\right) \\ &= W_N^{kM}\sum_{n=0}^{N-1} x(n-m)\exp\left(\frac{-j2\pi k(n-m)}{N}\right) = W_N^{kM}\sum_{r=-m}^{N-1-m} x(r)\exp\left(\frac{-j2\pi kr}{N}\right) \\ &= W_N^{kM}\sum_{r=0}^{N-1} x(r)\exp\left(\frac{-j2\pi kr}{N}\right) = W_N^{kM}X(k). \end{aligned} \tag{7.21}$$

Since $x(r)$ and $\exp(-2\pi jkr/N)$ both have period N, the summation over r in (7.21) may start at any index; in particular, if we start the summation at $r = 0$, we have precisely the DFT analysis formula for $X(k)$. The proof of the frequency shift property is similar and is left as an exercise. ■

Definition (Discrete Convolution). Let $x(n)$ and $y(n)$ be periodic signals with period $N > 0$. Then the signal $z(n)$ defined by

$$z(n) = \sum_{k=0}^{N-1} x(k)y(n-k) \tag{7.22}$$

is called the *discrete convolution* of x and y: $z = x * y$.

Note that the definition of discrete convolution can be extended to the case where one of the signals (or both) is not periodic. The expression (7.22) is computed for the periodic extension of the signals over $[0, N-1]$. We then have the following theorem that relates convolutions of discrete signals to the termwise products of their DFTs. Although we are working with frequency transforms of a greatly different formal nature, the comparison to the analog Fourier transform's Convolution Theorem is striking.

Theorem (Convolution in Time). Let $x(n)$ and $y(n)$ be periodic signals with period $N > 0$, $X(k)$ and $Y(k)$ their DFTs, and $z(n) = x * y$. Then the DFT of $z(n)$ is $Z(k) = X(k)Y(k)$.

Proof: A direct attack is fruitful. We write out the expression for $Z(k)$ according to the DFT analysis equation, insert the convolution formula for z in terms of x and y, and then separate the terms.

$$Z(k) = \sum_{n=0}^{N-1} z(n)W_N^{kn} = \sum_{n=0}^{N-1} (x*y)(n)W_N^{kn} = \sum_{n=0}^{N-1}\left(\sum_{m=0}^{N-1} x(m)y(n-m)\right)W_N^{kn}. \tag{7.23}$$

Interchanging the order of summation in (7.23) is the key step. This permits us to collect m-summation terms associated with x and n-summation terms associated with y together and expose the product of their DFTs.

$$\begin{aligned} Z(k) &= \sum_{m=0}^{N-1}\sum_{n=0}^{N-1} x(m)y(n-m)W_N^{kn} = \sum_{m=0}^{N-1} x(m)\sum_{n=0}^{N-1} y(n-m)W_N^{kn} \\ &= \sum_{m=0}^{N-1} x(m)W_N^{km}\sum_{n=0}^{N-1} y(n-m)W_N^{k(n-m)} = \sum_{m=0}^{N-1} x(m)W_N^{km}\sum_{r=0}^{N-1} y(r)W_N^{kr} = X(k)Y(k). \end{aligned} \tag{7.24}$$

We let $r = n - m$ for a change of summation variable in the penultimate summation of (7.24). Since $y(n)$ is periodic with period N, the summation from $r = -m$ to $N-1-m$ is the same as the summation from $r = 0$ to $N-1$. ■

Theorem (Convolution in Frequency). That is, let $x(n)$ and $y(n)$ be periodic signals with period $N > 0$; let $X(k)$ and $Y(k)$ be their DFTs, and let $z(n) = x(n)y(n)$ be the termwise product of x and y. Then the DFT of $z(n)$ is $Z(k) = (1/N)X(k)*Y(k)$, where $X(k)*Y(k)$ is the discrete convolution of $X(k)$ and $Y(k)$.

Proof: Similar to the Convolution in Time Theorem. ■

Proposition (Symmetry). Let signal $x(n)$ have period $N>0$ and $X(k)$ be its DFT. Then:

(a) The DFT of $x^*(n)$, the complex conjugate of $x(n)$, is $X^*(N-\mathrm{k})$, and the DFT of $x^*(N-n) = x^*(-n)$ is $X^*(k)$.
(b) The DFT of $x_e(n) = (1/2)(x(n) + x^*(N-n))$, the even part of $x(n)$, is $\mathrm{Re}[X(k)]$, the real part of $X(k)$.
(c) The DFT of $x_o(n) = (1/2)(x(n) - x^*(N-n))$, the odd part of $x(n)$, is $j\mathrm{Im}[X(k)]$, where Im[X(k)] is the imaginary part of $X(k)$.
(d) The DFT of $\mathrm{Re}[x(n)]$ is $X_e(k) = (1/2)(X(k) + X^*(N-k))$, the even part of $X(k)$.
(e) The DFT of $j\mathrm{Im}[x(n)]$ is $X_o(k) = (1/2)(X(k) - X^*(N-\mathrm{k}))$, the odd part of $X(k)$.

Proof: Easy. ■

Proposition (Real Signals). Let signal $x(n)$ be real-valued with period $N > 0$, and let $X(k)$ be its DFT. Then:

(a) $X(k) = X^*(N-k)$.
(b) The DFT of $x_e(n)$ is $\mathrm{Re}[X(k)]$.
(c) The DFT of $x_o(n)$ is $j\mathrm{Im}[X(k)]$.

Proof: Also easy. ■

Theorem (Parseval's). Let $x(n)$ have period $N > 0$ and let $X(k)$ be its DFT. Then

$$\sum_{m=0}^{N-1} x(n)\overline{x}(n) = \frac{1}{N}\sum_{k=0}^{N-1} X(k)\overline{X}(k). \tag{7.25}$$

Proof: Although it seems to lead into a messy triple summation, here again a stubborn computation of the frequency-domain energy for $X(k)$ on the interval $[0, N-1]$ bears fruit. Indeed,

$$\begin{aligned}
\sum_{k=0}^{N-1} X(k)\overline{X}(k) &= \sum_{k=0}^{N-1}\left(\sum_{m=0}^{N-1} x(m)W_N^{km}\right)\overline{\left(\sum_{n=0}^{N-1} x(n)W_N^{kn}\right)} \\
&= \sum_{k=0}^{N-1}\left(\sum_{m=0}^{N-1} x(m)W_N^{km}\right)\left(\sum_{n=0}^{N-1} \overline{x(n)}\,\overline{W_N^{kn}}\right) \\
&= \sum_{k=0}^{N-1}\sum_{m=0}^{N-1}\sum_{n=0}^{N-1} x(m)\overline{x(n)}W_N^{k(m-n)} \\
&= \sum_{m=0}^{N-1}\sum_{n=0}^{N-1} x(m)\overline{x(n)}\sum_{k=0}^{N-1} W_N^{k(m-n)}.
\end{aligned} \tag{7.26}$$

The last summation at the bottom in (7.26) contains a familiar expression: the partial geometric series in $(W_N)^{m-n}$ of length N. Recall from the lemma within the proof of the DFT Inverse Theorem (Section 7.1.1.1) that this term is either N or 0, according to whether $m = n$ or not, respectively. Thus, the only products $x(m)x^*(n)$ that will contribute to the triple sum in (7.26) are those where $m = n$, and these are scaled by the factor N. Therefore,

$$\sum_{k=0}^{N-1} X(k)\overline{X}(k) = \sum_{m=0}^{N-1}\sum_{n=0}^{N-1} x(m)\overline{x(n)}\sum_{k=0}^{N-1} W_N^{k(m-n)} = N\sum_{n=0}^{N-1} x(n)\overline{x(n)}, \tag{7.27}$$

and the proof is complete. ■

We have explored some of the theory of the DFT, noted its specific relation to the analog Fourier series, and considered its application for finding the significant periodicities in naturally occurring signals. In particular, we presented an example that uncovered the period of the sunspot cycle by taking the DFT of the discrete signal giving Wolf sunspot numbers over several centuries. We know from Chapter 4's attempts to analyze signals containing significant periodicities (textures, speech, tone detection, and the like) that pure time-domain methods—such as statistical approaches—can prove quite awkward. We do need the DFT for computer implementation, and the next section explores, therefore, the efficient computation of the DFT on digital computers.

7.1.4 Fast Fourier Transform

The fast Fourier transform (FFT) has been known, it turns out, since the time of Gauss.[3] Only recently, however, has it been widely recognized and utilized in signal processing and analysis. Indeed, its original rediscovery in the 1960s marks the beginning of an era in which digital methods supplanted analog methods in signal theory and applications.

7.1.4.1 Computational Cost. Let us begin by studying the computational costs incurred in the DFT analysis and synthesis equations. Clearly, if the time-domain signal, $x(n)$ on $[0, N-1]$, is complex-valued, then the operations are nearly identical. The IDFT computation requires an additional multiplication of a complex value by the factor $(1/N)$, as an inspection of the equations shows:

$$X(k) = \sum_{n=0}^{N-1} x(n)\exp\left(\frac{-2\pi jnk}{N}\right) = \sum_{n=0}^{N-1} x(n)W_N^{nk}, \tag{7.28a}$$

$$x(n) = \frac{1}{N}\sum_{k=0}^{N-1} X(k)\exp\left(\frac{2\pi jnk}{N}\right) = \frac{1}{N}\sum_{k=0}^{N-1} X(k)W_N^{-nk}. \tag{7.28b}$$

[3]Gauss, writing in a medieval form of Latin, made progress toward the algorithm in his notebooks of 1805. [M. T. Heideman, D. H. Johnson, and C. S. Burrus, 'Gauss and the history of the fast Fourier transform,' *IEEE ASSP Magazine*, vol. 1, no. 4, pp. 14–21, October 1984.]

But the principal computational burden lies in computing the complex sum of complex products in (7.28a) and (7.28b).

Consider the computation of $X(k)$ in (7.28a). For $0 \le k \le N-1$, the calculation of $X(k)$ in (7.28a) requires N complex multiplications and $N-1$ complex sums. Computing all N of the $X(k)$ values demands N^2 complex multiplications and $N^2 - N$ complex additions. Digital computers implement complex arithmetic as floating point operations on pairs of floating point values. Each complex multiplication, therefore, requires four floating point multiplications and two floating point additions; and each complex addition requires two floating point additions. So the total floating point computation of an N-point FFT computation costs $4N^2$ multiplications and $2(N^2 - N) + 2N^2$ additions. Other factors to consider in an FFT implementation are:

- Storage space and memory access time for the $x(n)$ and $X(k)$ coefficients;
- Storage space and memory access time for the $(W_N)^{kn}$ values;
- Loop counting and termination checking overheads.

Ultimately, as N becomes large, however, the number of floating point additions and multiplications weighs most significantly on the time to finish the analysis equation. Since the number of such operations—whether they are complex operations or floating point (real) operations—is proportional to N^2, we deem the DFT an order-N^2, or $O(N^2)$ operation.

FFT algorithms economize on floating point operations by eliminating duplicate steps in the DFT and IDFT computations. Two properties of the phase factor, W_N, reveal the redundancies in the complex sums of complex products (7.28a) and (7.28b) and make this reduction in steps possible:

- Phase factor periodicity: $(W_N)^{kn} = (W_N)^{k(n+N)}$;
- *Phase factor symmetry:* $[(W_N)^{kn}]^* = (W_N)^{k(N-n)}$.

Two fundamental approaches are decimation-in-time and decimation-in-frequency.

7.1.4.2 Decimation-in-Time. Decimation-in-time FFT algorithms reduce the DFT into a succession of smaller and smaller DFT analysis equation calculations. This works best when $N = 2^p$ for some $p \in \mathbb{Z}$. The N-point DFT computation resolves into two (N/2)-point, each of which resolves into two (N/4)-point DFTs, and so on.

Consider, then, separating the computation of $X(k)$ in (7.28a) into even and odd n within $[0, N-1]$:

$$\begin{aligned} X(k) &= \sum_{m=0}^{(N/2)-1} x(2m) W_N^{2km} + \sum_{m=0}^{(N/2)-1} x(2m+1) W_N^{(2m+1)k} \\ &= \sum_{m=0}^{(N/2)-1} x(2m) W_N^{2km} + W_N^k \sum_{m=0}^{(N/2)-1} x(2m+1) W_N^{2km} \end{aligned} \tag{7.29}$$

Note the common $(W_N)^{2km}$ phase factor in both terms on the bottom of (7.29). This leads to the key idea for the DFT's time-domain decimation:

$$W_N^2 = \exp\left(\frac{-2\pi j}{N}\right)^2 = \exp\left(\frac{-4\pi j}{N}\right) = \exp\left(\frac{-2\pi j}{N/2}\right) = W_{\left(\frac{N}{2}\right)}. \tag{7.30}$$

We set $y(m) = x(2m)$ and $z(m) = x(2m + 1)$. Then $y(m)$ and $z(m)$ both have period $N/2$. Also, (7.30) allows us to write (7.29) as a sum of the $N/2$-point DFTs of $y(m)$ and $z(m)$:

$$X(k) = \sum_{m=0}^{(N/2)-1} y(m) W_{\left(\frac{N}{2}\right)}^{km} + W_N^k \sum_{m=0}^{(N/2)-1} z(m) W_{\left(\frac{N}{2}\right)}^{km} = Y(k) + W_N^k Z(k). \tag{7.31}$$

From (7.31) it is clear that an N-point DFT is the computational equivalent of two $N/2$-point DFTs, plus $N/2$ complex multiplications, plus $N/2$ complex additions. Figure 7.5 illustrates the process of decomposing an 8-point DFT into two 4-point DFTs.

Does this constitute a reduction in computational complexity? The total cost in complex operations is therefore $2(N/2)^2 + 2(N/2) = N + N^2/2$ complex operations. For large N, the $N^2/2$ term, representing the DFT calculations, dominates. But the division by two is important! Splitting the $Y(k)$ and $Z(k)$ computations in the same way reduces the computation of the two DFTs to four $N/4$-point DFTs, plus $2(N/4)$ complex multiplications, plus $2(N/4)$ complex additions. The grand total cost

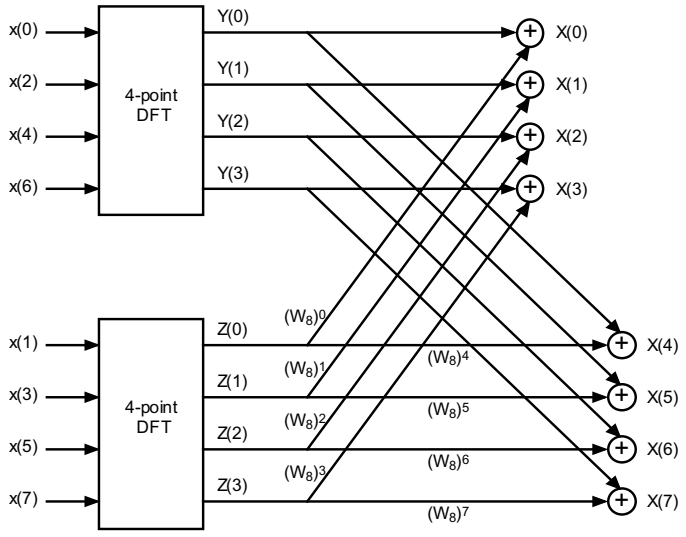

Fig. 7.5. The time domain decimation of an 8-point DFT. An 8-point analysis problem decomposes into two preliminary 4-point problems, followed by a scalar multiplication and a summation. This is only the first stage, but it effectively halves the number of complex operations necessary for computing the DFT of $x(n)$ on [0, 7].

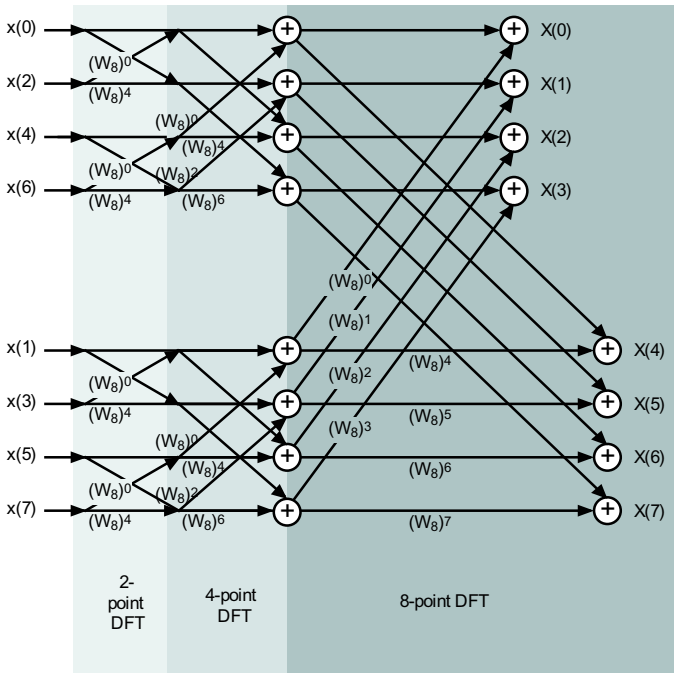

Fig. 7.6. Fully decimated 8-point DFT. Further decomposition steps expose an elementary operation that recurs throughout the computation. Notice also that the original data elements must be sorted in bit-reversed order at the beginning of the algorithm. Binary index numbers are used; that is, $x(000)$ is followed by $x(100)$, instead of $x(001)$, with which it swaps places. Next comes $x(010)$, since its bit-reversed index stays the same. But the next signal value must be $x(110)$, which swaps places with $x(011)$. This computational trick allows the in-place computation of DFT coefficients.

$N + [N + 4(N/4)^2] = N + N + N^2/4 = 2N + N^2/4$. The next iteration trims the cost to $3N + N^2/8$. And this can continue as long as N contains factors of two—$\log_2 N$ times. Thus, the fully executed decimation-in-time reduces the computational burden of an N-point DFT from $O(N^2)$ to $O(N\log_2 N)$.

Figure 7.6 illustrates the process of decomposing an 8-point DFT down to the final 2-point problem.

It turns out that a single basic operation underlies the entire FFT algorithm. Consider the 8-point problem in Figure 7.6. It contains three DFT computation stages. Four two-point problems comprise the first stage. Let us examine the structure of the first stage's operation. Pairs of the original signal elements are multiplied by either $(W_8)^0 = 1$ or $(W_8)^4 = -1$, as shown in Figure 7.7a. Thereafter, pairs of the two-point DFT coefficients are similarly multiplied by either of two possible powers of W_8: $(W_8)^0 = 1$ or $(W_8)^4 = -1$ again, or, $(W_8)^2$ and $(W_8)^6$.

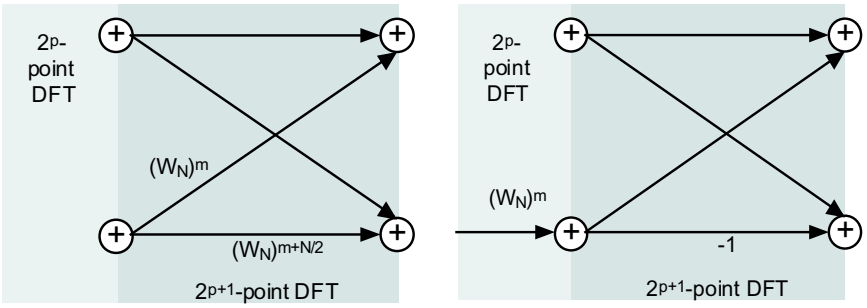

(a) (b)

Fig. 7.7. (a), The butterfly operation or its equivalent, simpler form (b), occurs throughout the FFT computation.

Indeed, at any of the later stages of computation, the multiplying phase factors always assume the form $(W_8)^m$ and $(W_8)^{m+4}$. Because their ratio is $(W_8)^{m+4-m} = (W_8)^4 = -1$, we may further simplify the rudimentary operation (Figure 7.7b), eliminating one complex multiplication. The resulting crisscross operation is called a butterfly, which the flow graph vaguely resembles. Some aesthetically pleasing term does seem appropriate: The butterfly operation reveals an elegant structure to the DFT operation, and the algorithms in Section 7.1.4.4 make efficient use of this elegance.

Now let us consider the rearrangement of the original signal values $x(0)$, $x(1)$, $x(2)$, $x(3)$, $x(4)$, $x(5)$, $x(6)$, $x(7)$ into the proper order for the four initial butterflies: $x(0)$, $x(4)$, $x(2)$, $x(6)$, $x(1)$, $x(5)$, $x(3)$, $x(7)$. This represents a bit-reversed reading of the indices of the data, because we observe that if the indices of the signal values are written in binary form, that is, $x(0) = x(000)$, $x(1) = x(001)$, and so on, then the necessary rearrangement comes from reading the binary indices backwards: $x(000)$, $x(100)$, $x(010)$, $x(110)$, $x(001)$, $x(101)$, $x(011)$, $x(111)$. At each of the three stages of the computation, we maintain eight complex values, beginning with the original signal data in bit-reversed order. Then we perform butterfly operations, with the index difference between value pairs doubling at each stage.

Now let us consider another approach to the efficient computation of the DFT by splitting the frequency domain values $X(k)$ into smaller and smaller groups.

7.1.4.3 Decimation-in-Frequency. Suppose again that we are faced with the problem of computing the DFT coefficients $X(k)$ for a signal $x(n)$ on $[0, N-1]$. In the previous section, we split the DFT analysis equation sum over $0 \le n \le N-1$ into two sums: for n even and for n odd. Now we divide the frequency-domain values $X(k)$ for $0 \le k \le N-1$ into even k and odd k. The result is an alternative, efficient algorithm for computing DFT coefficients called the decimation-in-frequency FFT.

Again, suppose that N is a power of 2, and let us consider DFT coefficients $X(k)$ where $k = 2m$. We have

$$\begin{aligned} X(2m) &= \sum_{n=0}^{N-1} x(n)W_N^{2mn} = \sum_{n=0}^{(N/2)-1} x(n)W_N^{2mn} + \sum_{n=N/2}^{N-1} x(n)W_N^{2mn} \\ &= \sum_{n=0}^{(N/2)-1} x(n)W_N^{2mn} + \sum_{n=0}^{(N/2)-1} x\left(n+\frac{N}{2}\right)W_N^{2m(n+\frac{N}{2})} \end{aligned} \tag{7.32}$$

Not unexpectedly, phase factor properties fortuitously apply. We observe that $(W_N)^{2m(n+N/2)} = (W_N)^{2mn}(W_N)^{mN} = (W_N)^{2mn}\,(W_{N/2})^{mn}$. Hence, for $0 \le m < N/2$, we have

$$\begin{aligned} X(2m) &= \sum_{n=0}^{(N/2)-1} x(n)W_N^{2mn} + \sum_{n=0}^{(N/2)-1} x\left(n+\frac{N}{2}\right)W_N^{2m(n+\frac{N}{2})} \\ &= \sum_{n=0}^{(N/2)-1} x(n)W_{N/2}^{mn} + \sum_{n=0}^{(N/2)-1} x\left(n+\frac{N}{2}\right)W_{N/2}^{2mn} \\ &= \sum_{n=0}^{(N/2)-1} \left[x(n)+x\left(n+\frac{N}{2}\right)\right]W_{N/2}^{2mn}. \end{aligned} \tag{7.33}$$

This last result shows that the $X(k)$ coefficients, for k even, can be calculated by an $(N/2)$-point DFT. Turning to the remaining $X(k)$, for $k = 2m + 1$ odd, we find

$$\begin{aligned} X(2m+1) &= \sum_{n=0}^{(N/2)-1} x(n)W_N^{(2m+1)n} + \sum_{n=N/2}^{N-1} x(n)W_N^{(2m+1)n} \\ &= \sum_{n=0}^{(N/2)-1} x(n)W_N^{(2m+1)n} + \sum_{n=0}^{(N/2)-1} x\left(n+\frac{N}{2}\right)W_N^{(2m+1)(n+N/2)} \\ &= \sum_{n=0}^{(N/2)-1} x(n)W_N^{(2m+1)n} + W_N^{(2m+1)(N/2)} \sum_{n=0}^{(N/2)-1} x\left(n+\frac{N}{2}\right)W_N^{(2m+1)n} \end{aligned} \tag{7.34}$$

Now it is time to invoke the phase factor properties: $(W_N)^{(2m\,+\,1)(n\,+\,N/2)} = (W_N)^{2mn}(W_N)^{m(N/2)} = -1$. Therefore, (7.34) simplifies to

$$
\begin{aligned}
X(2m+1) &= \sum_{n=0}^{(N/2)-1} x(n) W_N^{(2m+1)n} - \sum_{n=0}^{(N/2)-1} x\left(n+\frac{N}{2}\right) W_N^{(2m+1)n} \\
&= \sum_{n=0}^{(N/2)-1} \left[x(n) - x\left(n+\frac{N}{2}\right) \right] W_N^{(2m+1)n} \\
&= \sum_{n=0}^{(N/2)-1} \left[x(n) - x\left(n+\frac{N}{2}\right) \right] W_N^{2mn} W_N^n \\
&= \sum_{n=0}^{(N/2)-1} \left[x(n) - x\left(n+\frac{N}{2}\right) \right] W_{N/2}^{mn} W_N^n \\
&= \sum_{n=0}^{(N/2)-1} \left[W_N^n \left\{ x(n) - x\left(n+\frac{N}{2}\right) \right\} \right] W_{N/2}^{mn}.
\end{aligned} \tag{7.35}
$$

This shows that we can calculate $X(k)$ for k odd by an $(N/2)$-point DFT of the complex signal $y(n) = (W_N)^n[x(n) - x(n + (N/2))]$. Together (7.33) and (7.35) demonstrate that an N-point DFT computation can be replaced by two $(N/2)$-point DFT computations. As in the decimation-in-time strategy, we can iterate this divide-and-compute strategy as many times as N is divisible by two. The decimation-in-frequency result is an $O(N\log_2 N)$ algorithm too.

7.1.4.4 Implementation. This section considers FFT implementation in a modern high-level language, C++, and in assembly language on a representative digital signal processor, the Motorola 56000/56001.

Let's examine a C++ implementation of a radix-2 decimation-in-time algorithm, drawn from a classic FORTRAN coding of the FFT [4]. This algorithm uses the new standard template library contained in the header file <complex>. It replaces the traditional C++ complex arithmentic library, <complex.h>, which defines complex numbers as instances of a class whose member variables are two double-precision floating point numbers. The new template library allows us to construct complex numbers using the C++ float data type, for example, by declaring:

```
complex<float> x;
```

Specifying the `float` data type in the template conserves memory space.

Figure 7.8 shows the C++ implementation of the FFT.

Most references present FFT algorithms in FORTRAN [6–8], but also in C [9, 10]. The FFT can be implemented on a special computer architecture—called a shuffle-exchange network—that interconnects multiple processors in a manner similar to the FFT's butterfly flow diagram. This facilitates either the butterfly operation or the bit-reversed ordering of data, but not both at once, because interprocessor communication bottlenecks occur. Nevertheless, it is still possible to improve the FFT algorithm by an additional $O(N^{1/2})$ [11].

```
#include <math.h>
#include <stdlib.h>
#define PI 3.14159265358979
#include <use_ansi.h>
#include <complex>     //ISO/ANSI std template library
using namespace std;
int fft(complex<double> *x, int nu)
{ // sanity check to begin with:
  if (x == NULL || nu <= 0)
    return 0;
  int N = 1 << nu;          //N=2**nu
  int halfN = N >> 1;       //N/2
  complex<double> temp, u, v;
  int i, j, k;
  for (i = 1, j = 1; i < N; I++){  //bit-reversing data:
    if (i < j){ temp = x[j-1]; x[j-1] = x[i-1]; x[i-1] = temp;}
    k = halfN;
    while (k < j){j -= k; k >>= 1;}
    j += k;
  }
  int mu, M, halfM, ip;
  double omega;
  for (mu = 1; mu <= nu; mu++) {
    M = 1 << mu;      // M = 2**mu
    halfM = M >> 1;   // M/2
    u = complex<double>(1.0, 0.0);
    omega = PI/(double)halfM;
    w = complex<double>(cos(omega), -sin(omega));
    for (j = 0; j < halfM;j++){
      for (i = j; i < N; i += M){
        ip = i + halfM;
        temp = x[ip]*u;
        x[ip] = x[i] - temp;
        x[i] += temp;
      }
      u  *= w;
    }
    u  *= w;
  }
  return 1;
}
```

Fig. 7.8. A C++ implementation of the FFT. This algorithm uses the complex data type in the ISO/ANSI standard template library [5].

```
;Radix-2 decimation in time FFT macro call
fftr2a    macro points, data, coeff
          move #points/2, n0
          move #1,n2
          move #points/4, n6
          move #-1,m0
          move m0,m1
          move m0,m4
          move m0,m5
          move #0,m6              ; addr mod for bit-rev addr
          do   #@cvi (@log (points)/@log(2)+0.5),_end_pass
          move #data,r0
          move r0,r4
          lua  (r0)+n0,r1
          move #coef,r6
          lua  (r1)-,r5
          move n0,n1
          move n0,n4
          move n0,n5
          do   n2,_end_grp
          move x:(r1),x1    y:(r6),y0  ;sin and cos tables
          move x:(r5),a     y:(r6),b   ;load data values
          move x:(r6)+n6,x0
          do   n0,_end_bfy
          mac  x1,y0,b      y:(r1)+,y1 ;decim in time begins
          macr -x0,y1,b     a:x:(r5)+  y:(r0),a
          subl b,a          x:(r0),b   b,y: (r4)
          mac  -x1,x0,b     x:(r0)+,a  a,y: (r5)
          macr -y1,y0,b     x:(r1),x1
          subl b,a          b,x:(r4)+  y:(r0),b
_end_bfy
          move a,x:(r5)+n5       y:(r1)+n1,y1
          move x:(r0)+n0,x1      y:(r1)+n1,y1
_end_grp
          move n0,b1             ; div bfys/group by 2
          lsr  b            n2,a1
          lsl  a            b1,n0
          move a1,n2
_end_pass
          endm
```

Fig. 7.9. An Assembly language implementation of the FFT on the Motorala 56001 DSP chip [12]. The *X* and *Y* memory banks contain the input data's real and imaginary components, respectively. The *X* and *Y* memory banks also hold the cosine and sine tables for the exponential function implementation. The algorithm bit-reverses the output data stream.

It is interesting to examine the implementation of the FFT on a DSP processor (Figure 7.9). Let us now briefly describe some architectural features of this processor that support the implementation of digital signal processing algorithms. These features include:

- Multiple memory areas (X and Y) and data paths for two sets of signal data.
- No-overhead loop counting.
- A multiply-accumulate operation that runs in parallel with X and Y data movements.
- Built-in sine and cosine tables (in the case of the 56001) to avoid trigonometric function library calls.
- Addressing modes that support memory indexing needed for convolution operations.

The FFT code in Figure 7.9 explois these processing features for a compact implementation of decimation-in-time algorithm.

There are also FFT algorithms for $N \neq 2^n$. These general radix algorithms are more complicated, consume more memory space, and are less speedy than the dyadic decimation-in-time and decimation-in-frequency computations. Nevertheless, they are superior to the DFT and useful when the success of an application depends on fast frequency component computations. Another method, Goertzal's algorithm, uses a convolutional representation of the DFT's analysis equation as the basis for a fast computation. This algorithm is attractive for digital signal processors, because of their special hardware. Some of the exercises explore these FFT algorithms.

7.2 DISCRETE-TIME FOURIER TRANSFORM

In our study of signals and their frequency-domain representations, we have yet to cover one possibility: the class of discrete aperiodic signals. The frequency transform tool that applies to this case is the discrete-time Fourier transform (DTFT). It turns out that not all aperiodic discrete signals have DTFTs. We demonstrate that the transform exists for the important classes of absolutely summable and square-summable signals.

There is a generalization of the DTFT—the z-transform—which provides additional analytical capabilities suitable for those signals for which there is no DTFT. We cover the z-transform in Chapter 8. Chapter 9 explains a variety of applications of both the DTFT and the z-transform.

7.2.1 Introduction

We start the discussion with a formal definition—the mathematician's style at work once again. The definition involves an infinite sum, and so, as with the Fourier transform's infinite integral, for a given signal there are questions of the validity of the transform operation. We momentarily set these concerns aside to review a few examples. Then we turn to the important question of when the DTFT sum converges

and prove an inversion result. The DTFT is an important theoretical tool, since it provides the frequency domain characterization of discrete signals from the most important signal spaces we know from Chapter 2: the absolutely summable (l^1) signals and the square summable (l^2) signals.

7.2.1.1 Definition and Examples. Let us begin with the abstract definition of the DTFT and follow it with some simple examples. These provide some indication of the transform's nature and make the subsequent theorems more intuitive. The DTFT's definition does involve an infinite sum; for a given signal, therefore, we must eventually provide answers to existential questions about this operation.

Definition (Discrete-Time Fourier Transform). If $x(n)$ is a discrete signal, then the analog signal discrete signal $X(\omega)$ defined by

$$X(\omega) = \sum_{n=-\infty}^{+\infty} x(n) \exp(-jn\omega), \tag{7.36}$$

where $\omega \in \mathbb{R}$, is the *radial discrete-time Fourier transform* (DTFT) of $x(n)$. The units of ω are radians/second. We often refer to (7.36) as the DTFT analysis equation for $x(n)$. If we take $\omega = 2\pi f$, then we can define the (Hertz) DTFT also:

$$X(f) = \sum_{n=-\infty}^{+\infty} x(n) \exp(-j2\pi nf). \tag{7.37}$$

Generally, here, and in most texts, the DTFT takes the form (7.36) and, unless otherwise specified, we use the radial form of the transform.

Like the analog Fourier series, the DTFT is a transform that knows not what world it belongs in. The Fourier series, we recall from Chapter 4, transforms a periodic analog signal, $x(t)$, into a discrete signal: the Fourier coefficients $c(k) = c_k$. And the DTFT maps a discrete signal, $x(n)$, to an analog signal, $X(\omega)$. This prevents the FS and the DTFT from being considered bona fide systems. Both the Fourier transform and the DFT, however, can be viewed as systems. The FT maps analog signals to analog signals, and it may be considered a partial function on the class of analog signals. We know from Chapter 4's study of the FT that the absolutely integrable (L^1) signals, for example, are in the domain of the the FT system. Also, the DFT maps discrete signals of period N to discrete signals of period N. We surmise (rightly, it turns out) that, owing to the doubly infinite sum in the analysis equation, the study of the DTFT will involve much more mathematical subtlety than the DFT.

Clearly, the DTFT sum exists whenever the signal $x(n)$ is finitely supported; that is, it is zero outside some finite interval. So for a wide—and important—class of signals, the DTFT exists. Without worrying right now about the convergence of the analysis equation (7.36) for general signals, we proceed to some examples of the radial DTFT.

Example (Discrete Delta Signal). Consider the signal $\delta(n)$, the discrete delta function. This signal is unity at $n = 0$, and it is zero for $n \neq 0$. For any $\omega \in \mathbb{R}$, all of the summands in (7.36) are zero, save the $n = 0$ term, and so we have $X(\omega) = 1$ for all $\omega \in \mathbb{R}$.

Example (Discrete Square Pulse). Consider the signal $h(n) = [1, 1, \underline{1}, 1, 1]$, which is unity for $-2 \leq n \leq 2$ and zero otherwise. We recognize this signal as the impulse response of a Moving Average System. If $y = Hx = h * x$, then the system H averages the five values around $x(n)$ to produce $y(n)$. We calculate

$$\begin{aligned} H(\omega) &= \sum_{n=-\infty}^{+\infty} h(n)\exp(-jn\omega) = \sum_{n=-2}^{+2} \exp(-jn\omega) \\ &= e^{2j\omega} + e^{j\omega} + 1 + e^{-j\omega} + e^{-2j\omega} = 1 + 2\cos(\omega) + 2\cos(2\omega). \end{aligned} \tag{7.38}$$

The notation might cause confusion, but we will use $H(\omega)$ for the DTFT of discrete signal $h(n)$ and simply H for the system with impulse response $h(n)$. Figure 7.10 plots $H(\omega)$.

Example (Exponential Signal). Consider the signal $x(n) = 2^{-n}u(n)$, and its DTFT analysis equation,

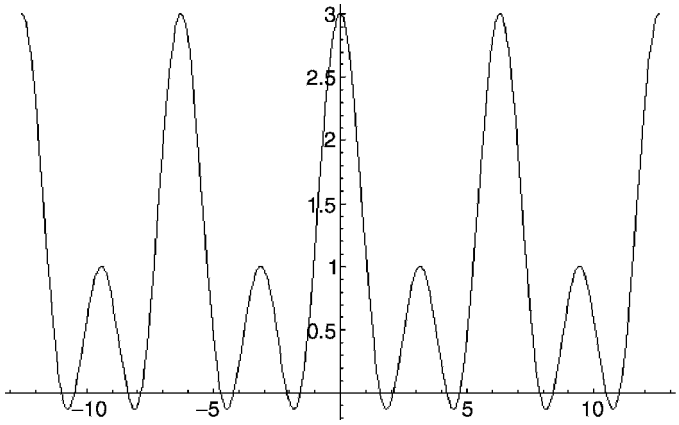

Fig. 7.10. Graph of $H(\omega)$ where $h(n) = [1, 1, \underline{1}, 1, 1]$. $H(\omega)$ is a 2π-periodic analog signal, and it assumes a maximum value at $\omega = 0$. In general, $H(\omega)$ is complex, and in such cases we prefer to plot $|H(\omega)|$ and $\arg(H(\omega))$ on one period: $[0, 2\pi]$ or $[-\pi, \pi]$.

$$X(\omega)=\sum_{n=-\infty}^{+\infty}x(n)\exp(-jn\omega)=\sum_{n=0}^{+\infty}\left(\frac{1}{2}\right)^n\exp(-jn\omega)=\sum_{n=0}^{+\infty}\left(\frac{e^{-j\omega}}{2}\right)^n$$

$$=\frac{1}{1-\left(\dfrac{e^{-j\omega}}{2}\right)}=\frac{1}{1-\dfrac{\cos(\omega)}{2}+j\dfrac{\sin(\omega)}{2}}=\frac{1-\dfrac{\cos(\omega)}{2}-j\dfrac{\sin(\omega)}{2}}{\left(1-\dfrac{\cos(\omega)}{2}\right)^2+\left(\dfrac{\sin(\omega)}{2}\right)^2}. \quad (7.39)$$

Signal $x(n)$ is a geometric series of the form $1 + a + a^2 + \cdots$, where $a = (1/2)\exp(-j\omega)$. Since $|a| = 1/2 < 1$, the step from an infinite sum to the simple quotient $1/(1 - a)$ on the bottom left side of (7.39) is justified. Figure 7.11 shows the magnitude and phase of the DTFT of $x(n)$.

Notice that the DTFT (7.36) appears to be in the form of an l^2 inner product. Given $x(n)$, we can informally write $X(\omega) = \langle x(n), \exp(j\omega n)\rangle$, because the l^2 inner

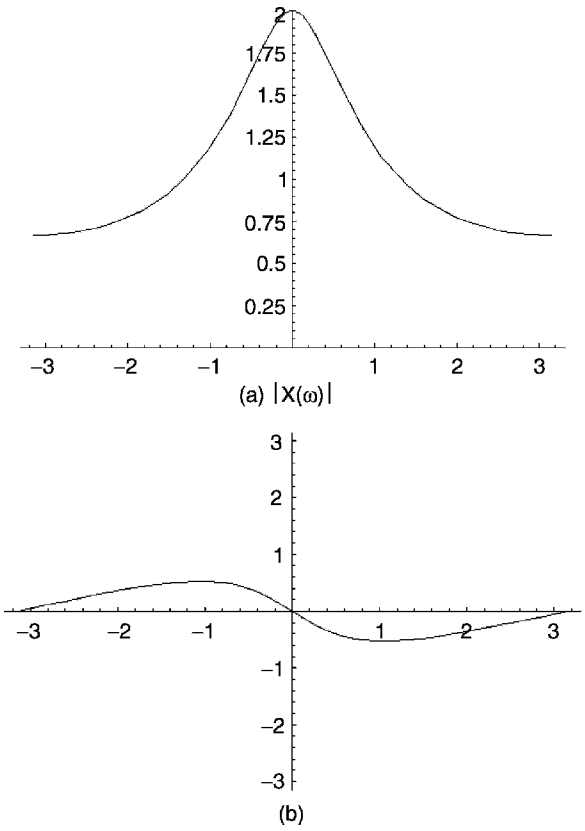

Fig. 7.11. DTFT of $x(n) = 2^{-n}u(n)$. Panel (a) shows $|X(\omega)|$ on $[-\pi, \pi]$. Panel (b) plots $\arg(X(\omega))$.

product, like the DTFT analysis equation, is precisely the sum of all products of terms $x(n)\exp(-j\omega n)$. Conceptually (and still informally), then, for each ω the DTFT $X(\omega)$ measures the similarity between $x(n)$ and $\exp(j\omega n)$. So $X(\omega)$ is the spectral content of the discrete signal $x(n)$ for radial frequency ω. We cannot formalize this intuition unless we know more about the convergence of the analysis equation sum. The signal $\exp(j\omega n)$ is not square-summable, so we do not know, without more investigation, whether the inner product-like sum converges. The convergence of the DTFT analysis equation is a question that we must therefore address, and fortunately, there are satisfactory answers.

7.2.1.2 Existence. Let us consider two of the most important classes of discrete signals: absolutely-summable signals and square-summable signals. Do representatives of these function spaces always have discrete-time Fourier transforms? Guaranteeing a transform for l^2 signals, like the case of the analog L^2 Fourier transforms in Chapter 5, requires some care. There is, however, a very easy existence proof for the DTFT of l^1 signals.

Theorem (DTFT Existence for Absolutely Summable Signals). Suppose $x(n) \in l^1$. Then the DTFT of $x(n)$, $X(\omega)$, exists and converges absolutely and uniformly for all $\omega \in \mathbb{R}$.

Proof: To show absolute convergence of the analysis equation, we need to show that

$$\sum_{n=-\infty}^{+\infty} \left|x(n)\exp(-jn\omega)\right| = \sum_{n=-\infty}^{+\infty} \left|x(n)\right|\left|\exp(-jn\omega)\right| = \sum_{n=-\infty}^{+\infty} \left|x(n)\right| < \infty. \tag{7.40}$$

But the last term in (7.40) is precisely the l^1 norm of $x(n)$, and this must be finite, since $x(n) \in l^1$. So the analysis equation formula for $X(\omega)$ does indeed converge to a limit for any ω. We recall from real and complex analysis [13, 14] that the uniform convergence of the series (7.36), means that for every $\varepsilon > 0$ there is an $N > 0$ such that if $m, n > N$, then for all ω:

$$\left|\sum_{k=m}^{k=n} x(k)\exp(-jk\omega)\right| < \varepsilon. \tag{7.41}$$

The main point of uniform convergence is that the Cauchy criterion (7.41) applies to all ω, independent of N, which depends only on the choice of ε. If N must vary with ε, then ordinary, but not uniform, convergence exists. Now, (7.40) shows convergence for all ω; the interval $[-\pi, \pi]$ is closed and bounded, hence it is *compact*; and a convergent series on a compact subset of the real line is uniformly convergent on that subset. Therefore, since we know that $X(\omega)$ is periodic with period $[-\pi, \pi]$, the DTFT analysis equation series converges uniformly to $X(\omega)$ for all ω. ■

Corollary (Continuity of DTFT). Suppose $x(n) \in l^1$. Then the DTFT of $x(n)$, $X(\omega)$, is continuous.

Proof: It is the sum of a uniformly convergent series, and each partial sum in the series,

$$S_N(\omega) = \sum_{n=-N}^{n=N} x(n)\exp(-jn\omega), \tag{7.42}$$

is a continuous function of ω. ■

Now consider a signal $x(n) \in l^2$. We are familiar with the signal space l^2 from Chapter 2: It is the Hilbert space of square-summable discrete signals. It has an inner product, $\langle x, y\rangle$, which measures how alike are two l^2 signals; a norm, $\|x\|_2$, which derives from the inner product, $\|x\|_2 = (\langle x, x\rangle)^{1/2}$; and orthonormal bases, $\{e_i : i \in \mathbb{N}\}$, which allow us to decompose signals according to their similarity to the basis elements, $\langle e_i, x\rangle$. Thus, Hilbert spaces extend the convenient analytical tools (which one finds, for example, in finite-dimensional vector spaces), to the doubly infinite "vectors" of signal processing and analysis—discrete signals. Let us next show that for square-summable signals the DTFT exists.

Theorem (DTFT Existence for Square-Summable Signals). Suppose $x(n) \in l^2$. Then the DTFT of $x(n)$, $X(\omega)$, exists for all $\omega \in \mathbb{R}$.

Proof: Let $\omega \in \mathbb{R}$ and consider the partial DTFT analysis equations sums,

$$X_N(\omega) = \sum_{n=-N}^{+N} x(n)\exp(-jn\omega), \tag{7.43}$$

where $N \in \mathbb{N}$, the natural numbers. (We shall use the notation $X_N(\omega)$ for DTFT partial sums quite a bit.) Let H be the Hilbert space of square-integrable analog signals (cf. Chapter 3) on $[-\pi, \pi]$: $H = L^2[-\pi, \pi]$. For each N, $X_N(\omega)$ has period 2π and is square-integrable on $[-\pi, \pi]$:

$$\left\|X_N(\omega)\right\|_H^2 = \int_{-\pi}^{\pi} \left| \sum_{n=-N}^{N} x(n)\exp(-jn\omega) \right|^2 d\omega < \infty; \tag{7.44}$$

hence, $X_N(\omega) \in L^2[-\pi, \pi]$. Let us denote the L^2-norm on H of a square-integrable signal, $s(t)$, by $\|s(t)\|_H$. We wish to show that $(X_N(\omega): N \in \mathbb{N})$ is an $L^2[-\pi, \pi]$ Cauchy sequence; that is, given $\varepsilon > 0$, we can choose $N > M$ both sufficiently large so that $\|X_N - X_M\|_H < \varepsilon$. This would imply that the limit of the sequence $(X_N(\omega))$, which is the series sum of the analysis equation for $x(n)$, does in fact converge to an element of H: $X(\omega)$. Note that

$$X_N(\omega) - X_M(\omega) = \sum_{n=M+1}^{N} x(n)\exp(-jn\omega) + \sum_{n=-M-1}^{-N} x(n)\exp(-jn\omega). \tag{7.45}$$

Thus, using the orthogonality of signals $\exp(-jwn)$ on $[-\pi, \pi]$ and the properties of the inner product on H, we find

$$
\begin{aligned}
&\left\|X_N(\omega)-X_M(\omega)\right\|_H^2 \\
&=\left\langle \sum_{n=M+1}^{N} x(n)e^{-j\omega n}+\sum_{n=-M-1}^{-N} x(n)e^{-j\omega n}, \sum_{m=M+1}^{N} x(m)e^{-j\omega m}+\sum_{m=-M-1}^{-N} x(m)e^{-j\omega m}\right\rangle \\
&=\left\langle \sum_{n=M+1}^{N} x(n)e^{-j\omega n}, \sum_{m=M+1}^{N} x(m)e^{-j\omega m}+\sum_{m=-M-1}^{-N} x(m)e^{-j\omega m}\right\rangle \\
&\quad+\left\langle \sum_{n=-M-1}^{-N} x(n)e^{-j\omega n}, \sum_{m=M+1}^{N} x(m)e^{-j\omega m}+\sum_{m=-M-1}^{-N} x(m)e^{-j\omega m}\right\rangle \\
&=\left\langle \sum_{n=M+1}^{N} x(n)e^{-j\omega n}, \sum_{m=M+1}^{N} x(m)e^{-j\omega m}\right\rangle+\left\langle \sum_{n=M+1}^{N} x(n)e^{-j\omega n}, \sum_{m=-M-1}^{-N} x(m)e^{-j\omega m}\right\rangle \\
&\quad+\left\langle \sum_{n=-M-1}^{-N} x(n)e^{-j\omega n}, \sum_{m=M+1}^{N} x(m)e^{-j\omega m}\right\rangle+\left\langle \sum_{n=-M-1}^{-N} x(n)e^{-j\omega n}, \sum_{m=-M-1}^{-N} x(m)e^{-j\omega m}\right\rangle \\
&=\sum_{n=M+1}^{N}\sum_{m=M+1}^{N} x(n)\bar{x}(m)\left\langle e^{-j\omega n}, e^{-j\omega m}\right\rangle+\sum_{n=M+1}^{N}\sum_{m=-M-1}^{-N} x(n)\bar{x}(m)\left\langle e^{-j\omega n}, e^{-j\omega m}\right\rangle \\
&\quad+\sum_{n=-M-1}^{-N}\sum_{m=M+1}^{N} x(n)\bar{x}(m)\left\langle e^{-j\omega n}, e^{-j\omega m}\right\rangle+\sum_{n=-M-1}^{-N}\sum_{m=-M-1}^{-N} x(n)\bar{x}(m)\left\langle e^{-j\omega n}, e^{-j\omega m}\right\rangle \\
&=2\pi\sum_{n=M+1}^{N} x(n)\bar{x}(n)+0+0+2\pi\sum_{n=-M-1}^{-N} x(n)\bar{x}(n). \qquad (7.46)
\end{aligned}
$$

We have used $\langle \exp(-j\omega n), \exp(-j\omega m)\rangle = 2\pi\delta_{n,m}$, where $\delta_{n,m}$ is the Kronecker delta, to simplify the first and last double summations and to discard the two middle double summations in (7.46). Now, since $x(n) \in l^2$, it has a finite l^2-norm; in other words,

$$\left\|x(n)\right\|^2 = \sum_{n=-\infty}^{\infty} x(n)\bar{x}(n) < \infty. \qquad (7.47)$$

This means that for $\varepsilon > 0$, we can find $N > M$ sufficiently large so that

$$\sum_{n=M+1}^{N} x(n)\bar{x}(n) < \varepsilon \qquad (7.48a)$$

and

$$\sum_{n=-M-1}^{-N} x(n)\bar{x}(n) < \varepsilon. \qquad (7.48b)$$

Together, (7.48a) and (7.48b) imply that (7.46) can be made arbitrarily small. Thus the sequence $(X_N(\omega): N \in \mathbb{N})$ is Cauchy in $H = L^2[-\pi, \pi]$. Since H is a Hilbert space, this Cauchy sequence converges to a signal, the DTFT of $x(n)$, $X(\omega) \in H$. ■

7.2.1.3 Inversion. This section studies the problem of finding an inverse for the DTFT. Those frequency transforms covered so far—the Fourier series, the Fourier transform, and the discrete Fourier transform—all have inverses, assuming, in the case of the FS and FT that our signals belong to certain function spaces. So we expect no exceptions from the frequency transform for discrete aperiodic signals. Now, the DTFT of a discrete signal $x(n)$ is a periodic function $X:\mathbb{R} \to \mathbb{C}$, so the inverse must transform a periodic analog signal into a discrete signal. One transform, familiar from Chapter 5, does precisely this—the Fourier series. For an analog periodic signal, the FS finds a discrete set of frequency coefficients. We shall see that there is in fact a very close relationship between the inverse relation for the DTFT and the analog FS.

Our first theorem provides a simple criterion for the existence of an inverse.

Theorem (Inverse DTFT). Suppose that $x(n)$ has a DTFT, $X(\omega)$, and that the analysis equation for $X(\omega)$ converges uniformly on $[-\pi, \pi]$. Then, for all $n \in \mathbb{Z}$,

$$x(n) = \frac{1}{2\pi} \int_{-\pi}^{+\pi} X(\omega) \exp(j\omega n)\, d\omega \cdot \tag{7.49}$$

Proof: The stipulation that the analysis equation's convergence be uniform is critical to the proof. The DTFT analysis equation for $x(n)$ is a limit of partial sums:

$$X(\omega) = \lim_{N\to\infty} X_N(\omega) = \lim_{N\to\infty} \sum_{n=-N}^{+N} x(n) \exp(-jn\omega) = \sum_{n=-\infty}^{+\infty} x(n) \exp(-jn\omega). \tag{7.50}$$

After changing the dummy summation variable, we insert (7.50) directly into the integrand of (7.49):

$$\frac{1}{2\pi} \int_{-\pi}^{+\pi} X(\omega) \exp(j\omega n)\, d\omega = \frac{1}{2\pi} \int_{-\pi}^{+\pi} \left(\lim_{N\to\infty} \sum_{m=-N}^{+N} x(m) \exp(-jm\omega) \right) \exp(j\omega n)\, d\omega. \tag{7.51}$$

The uniform convergence of the limit in (7.51) permits us to interchange the integration and summation operations [13]:

$$\begin{aligned} \frac{1}{2\pi} \int_{-\pi}^{+\pi} X(\omega) \exp(j\omega n)\, d\omega &= \frac{1}{2\pi} \lim_{N\to\infty} \sum_{m=-N}^{+N} x(m) \int_{-\pi}^{+\pi} \exp[j\omega(n-m)]\, d\omega \\ &= \frac{1}{2\pi} \sum_{m=-\infty}^{+\infty} x(m) \delta_{m,n} = x(n), \end{aligned} \tag{7.52}$$

where $\delta_{n,m}$ is the Kronecker delta. ■

Corollary (Inverse DTFT for Absolutely Summable Signals). If $x(n) \in l^1$, then for all $n \in \mathbb{Z}$,

$$x(n) = \frac{1}{2\pi} \int_{-\pi}^{+\pi} X(\omega) \exp(j\omega n)\, d\omega\,, \tag{7.53}$$

where $X(\omega)$ is the DTFT of $x(n)$.

Proof: The analysis equation sum for $X(\omega)$ converges uniformly by the DTFT Existence Theorem for Absolutely Summable Signals in the previous section. Hence the Inverse Theorem above implies that the formula (7.53) is valid. ■

Definition (Inverse Discrete-Time Fourier Transform). If $X(\omega)$ is a 2π-periodic analog signal and $x(n)$, as defined by (7.53), exists, then $x(n)$ is the *inverse discrete-time Fourier transform* (IDTFT) of $X(\omega)$. Equation (7.53) is also called the DTFT *synthesis equation*.

This last result (7.53) highlights an intriguing aspect of the DTFT. Equation (7.53) says that if $x(n)$ is absolutely summable, then $x(n)$ is the nth Fourier series coefficient for $X(\omega)$. To understand this, recall that if the analog signal $y(s) \in L^1[0, T]$ has period $T > 0$, then the Fourier series analysis equation gives (unnormalized) Fourier coefficients,

$$c_k = \frac{1}{T} \int_{-T/2}^{+T/2} y(s) \exp(-2\pi jkFs)\, ds, \tag{7.54}$$

where $F = 1/T$. The companion synthesis equation reconstructs $y(s)$ from the c_k:

$$y(s) = \sum_{k=-\infty}^{+\infty} c_k \exp(2\pi jkFs). \tag{7.55}$$

The reconstruction is not perfect, however. When $y(s)$ contains a discontinuity at $s = s_0$, then the synthesis equation converges to a value midway between the left- and right-hand limits of $y(s)$ at $s = s_0$. We can easily transpose (7.55) to the form of the DTFT analysis equation. We need only set $x(k) = c_k$, $\omega = -2\pi Fs$, and $X(\omega) = y(s) = y(-\omega/(2\pi F))$. Therefore, analog periodic signals have discrete spectral components given by the Fourier series coefficients. And discrete aperiodic signals have continuous periodic spectra given by their 2π-periodic DTFTs. There is more than an affinity between the discrete aperiodic signals and the analog periodic signals; there is, as we shall see in a moment, a Hilbert space isomorphism.

Now, we have found an inversion relation for the DTFT and defined the synthesis equation for absolutely summable signals, but what about l^2 signals? This is our most important l^p space, since it supports an inner product relation. Is there an

inverse relation similar to (7.53) for square-summable discrete signals? The following theorem helps to answer this question in the affirmative, and it is one step toward showing the essential sameness of l^2 and $L^2[-\pi, \pi]$.

Theorem (DTFT Existence for Square-Summable Signals). If $x(n) \in l^2$, then there is an analog signal $y(s) \in L^2[-\pi, \pi]$ such that

$$x(n) = \frac{1}{2\pi} \int_{-\pi}^{+\pi} y(s) \exp(jsn)\, ds, \tag{7.56a}$$

for all $n \in \mathbb{Z}$, and

$$y(s) = \sum_{n=-\infty}^{+\infty} x(n) \exp(-jsn), \tag{7.56b}$$

Proof: Recall the Riesz–Fischer Theorem from Chapter 2. Suppose we take $H = L^2[-\pi, \pi]$ as the Hilbert space and $\{e_n(s): n \in \mathbb{Z}\} = \{(2\pi)^{-1/2}\exp(-jsn): n \in \mathbb{Z}\}$ as the orthonormal set in H which Riesz–Fischer presupposes. Then the Riesz–Fischer result states that if $x(n) \in l^2$, then there is a $w(s) \in H$ such that $\langle w, e_n(s)\rangle = x(n)$, and $w = \Sigma x(n) e_n(s)$. Furthermore, w is unique in the following sense: Any other $h \in H$ for which this holds can differ from w only on a set of measure zero; in other words, $\|w - h\|_2 = 0$, where $\|\cdot\|_2$ is the norm on $L^2[-\pi, \pi]$:

$$\|y\|_2 = \left(\int_{-\pi}^{+\pi} |y(s)|^2 ds \right)^{\frac{1}{2}}. \tag{7.57}$$

Continuing to apply this previous abstract theorem to our present concrete problem, we must have a $w(s) \in H$ such that

$$x(n) = \langle w, e_n \rangle = \langle w, \exp(-jsn) \rangle = \int_{-\pi}^{+\pi} w(s) \frac{\exp(jsn)}{\sqrt{2\pi}}\, ds \tag{7.58}$$

and

$$w(s) = \sum_{n=-\infty}^{+\infty} x(n) e_n(s) = \sum_{n=-\infty}^{+\infty} x(n) \frac{\exp(-jsn)}{\sqrt{2\pi}}. \tag{7.59}$$

Setting $y(s) = (2\pi)^{1/2} w(s)$ completes the proof. ■

How exactly does this help us answer the question of whether square-summable discrete signals have DTFTs? Briefly, $x(n) \in l^2$ does have a DTFT: We take $X(\omega) = y(\omega)$, where y is the $L^2[-\pi, \pi]$ signal guaranteed by the theorem. The problem is that $X(\omega)$ need not be continuous; therefore, there are many possible choices for $X(\omega)$ in

$L^2[-\pi, \pi]$ that obey the DTFT synthesis equation. The various choices may differ on a set of measure zero, so that the norm of their difference, computed with an integral of adequate power (such as the Lebesgue integral) is zero. This should be no surprise. We recall Chapter 5's lesson, for example, that the Fourier series sum of a signal converges to the midpoint of a signal discontinuity. The FS imperfectly recovers the original periodic analog signal. If $x(n) \in l^1$, on the other hand, then the convergence of the DTFT analysis equation (or, alternatively, the convergence of the Fourier series sum) is uniform, so that $X(\omega)$ is continuous and pointwise unique on $[-\pi, \pi]$.

Corollary (Embedding of l^2 into $L^2[-\pi, \pi]$). For $x(n) \in l^2$, then set $\mathcal{F}(x) = (2\pi)^{-1/2}X(\omega) \in L^2[-\pi, \pi]$. Then $\mathcal{F}$ is a Hilbert space isomorphism between l^2 and (the equivalence classes of signals that are equal almost everywhere) its image $\mathcal{F}[l^2]$.

Proof: The theorem guarantees that a unique (up to a set of measure zero) $X(\omega)$ exists, so $\mathcal{F}$ is well-defined. It is also clear that the DTFT is a linear mapping from l^2 to $L^2[-\pi, \pi]$, and so too is $\mathcal{F}$ (exercise). We need to show as well that $\langle x, y\rangle = \langle \mathcal{F}x, \mathcal{F}y\rangle$, for all $x, y \in l^2$. Let $Y(\omega)$ be the DTFT of $y(n)$. Working from within the realm of $L^2[-\pi, \pi]$, we find

$$\begin{aligned}\langle X,Y\rangle &= \int_{-\pi}^{+\pi} X(\omega)\overline{Y}(\omega)\, d\omega = \int_{-\pi}^{+\pi}\left[\sum_{n=-\infty}^{+\infty} x(n)\exp(-j\omega n)\right]\left[\sum_{k=-\infty}^{+\infty} \overline{y}(k)\exp(j\omega k)\right] d\omega \\ &= \int_{-\pi}^{+\pi}\left[\sum_{n=-\infty}^{+\infty}\sum_{k=-\infty}^{+\infty} x(n)\overline{y}(k)\exp^{-j\omega(n-k)}\right] d\omega. \end{aligned} \tag{7.60}$$

Since $x, y \in l^2$, the partial sums $X_N(\omega)$ and $Y_N(\omega)$ converge absolutely; for example, we have $|x(n)\exp(-j\omega n)| = |x(n)|$, and $\Sigma|x(n)|^2 = (\|x\|_2)^2 < \infty$. This justifies the step to a double summation of products [13]. And, because the double sum on the bottom of (7.60) converges on the closed set $[-\pi, \pi]$, it converges uniformly. This allows us to interchange the summation and integration operations, obtaining

$$\begin{aligned}\langle X,Y\rangle &= \sum_{n=-\infty}^{+\infty}\sum_{k=-\infty}^{+\infty}\int_{-\pi}^{+\pi} x(n)\overline{y}(k)\exp^{-j\omega(n-k)}\, d\omega = 2\pi\sum_{n=-\infty}^{+\infty} x(n)\overline{y}(n) \\ &= 2\pi\langle x(n), y(n)\rangle. \end{aligned} \tag{7.61}$$

Only the terms with $n = k$ in the integral of (7.61) are nonzero. Finally, since $\mathcal{F}(x) = (2\pi)^{-1/2}X(\omega)$, $\langle \mathcal{F}x, \mathcal{F}y\rangle = \langle x, y\rangle$. ■

An embedding therefore exists from the discrete Hilbert space l^2 into the continuous Hilbert space $L^2[-\pi, \pi]$. This Hilbert subspace of $L^2[-\pi, \pi]$, the image of l^2 under $\mathcal{F}$, $\mathcal{F}[l^2]$, is essentially just like l^2. Is it the case, perhaps owing to the intricacies

of its analog signal elements, that the full Hilbert space, $L^2[-\pi, \pi]$, is fundamentally more complex than l^2? The requisite tools of formal analog theory—Dirac delta functions, Lebesgue integration, questions of separability, and so on—make it tempting to conclude that $L^2[-\pi, \pi]$ ought to be a richer mathematical object than the drab, discrete l^2. Moreover, the embedding that we have given is a straightforward application of the abstract Riesz–Fischer theorem; no technical arguments using the specific characteristics of $L^2[-\pi, \pi]$ signals are necessary. So it might well be concluded that the orthogonal complement, $\mathcal{F}[l^2]^{\perp}$, is indeed nontrivial.

No, the truth is quite the opposite: The mapping $\mathcal{F}(x(n)) = (2\pi)^{-1/2}X(\omega)$ from l^2 into $L^2[-\pi, \pi]$ is indeed a Hilbert space isomorphism. We can show this if we can find a set of signals in the image of l^2 under the embedding relation, $\mathcal{F}$, that is dense in $L^2[-\pi, \pi]$. In general, questions of orthogonality and finding embeddings (also called injections) of one Hilbert space into another tend to admit easier answers. But showing that one or another set of orthogonal elements spans the entire Hilbert space—the question of completeness—is quite often a daunting problem. Fortunately, we already have the crucial tool in hand, and the next corollary explains the result.

Corollary (Isomorphism of l^2 and $L^2(-\pi, \pi)$). Let $x(n) \in l^2$, let $X(\omega)$ be the DTFT of $x(n)$, and set $\mathcal{F}(x) = (2\pi)^{-1/2}X(\omega) \in L^2[-\pi, \pi]$. Then $\mathcal{F}$ is a Hilbert space isomorphism.

Proof: Consider some $Y(\omega) \in L^2[-\pi, \pi]$. We need to show that Y is arbitrarily close to some element of the image of $\mathcal{F}$, $\mathcal{F}[l^2]$. From Chapter 5, Y has a Fourier series representation,

$$\begin{aligned} Y(\omega) &= \sum_{k=-\infty}^{+\infty} c_k \exp(2\pi jkF\omega) = \sum_{k=-\infty}^{+\infty} c_k \exp(jk\omega) \\ &= \lim_{K\to\infty} \sum_{k=-K}^{+K} c_k \exp(jk\omega) = \lim_{K\to\infty} Y_K(\omega), \end{aligned} \tag{7.62}$$

where

$$c_k = \frac{1}{T}\int_{-T/2}^{+T/2} Y(\omega)\exp(-2\pi jkF\omega)\, d\omega = \frac{1}{2\pi}\int_{-\pi/2}^{+\pi/2} Y(\omega)\exp(-jk\omega)\, d\omega. \tag{7.63}$$

Since $T = \pi - (-\pi) = 2\pi$ and $F = 1/T = 1/(2\pi)$, (7.62) shows that see that $Y(\omega)$ is really the limit of the $Y_K(\omega)$. But each $Y_K(\omega)$ is a linear combination of exponentials, $\exp(jk\omega)$, which are in the image, $\mathcal{F}[l^2]$. Since Y was arbitrary, this implies that the span of the exponentials is dense in $L^2[-\pi, \pi]$, or, equivalently, that its closure is all of $L^2[-\pi, \pi]$. ■

The next section contains an extended study of a single example that illustrates some of the convergence problems that arise when taking the DTFT of a signal that is not absolutely summable.

7.2.1.4 Vagaries of $X(\omega)$ convergence in $L^2[-\pi, \pi]$. The search for those classes of discrete signals, $x(n)$, that have a DTFT leads to difficulties with the convergence of the analysis equation sum. We have just shown that absolutely summable and square-summable discrete signals have DTFTs; if $x(n) \in l^2$, however, we cannot guarantee that the DTFT, $X(\omega)$, is unique. Now we explore in some detail an example of a square-summable signal that is not in l^1. Its DTFT is not unique, due to the presence of discontinuities in $X(\omega)$. Moreover, its convergence is tainted by spikes near the points of discontinuity that persist even as the partial analysis equation sums converge (in the l^2 norm) to $X(\omega)$.

Example (Discrete Sinc Signal). Consider the signal $x(n)$ defined as follows:

$$x(n) = \frac{\operatorname{sinc}(n)}{\pi} = \begin{cases} \dfrac{\sin(n)}{\pi n} & \text{if } n \neq 0, \\ \dfrac{1}{\pi} & \text{if } n = 0. \end{cases} \tag{7.64}$$

Although $x(n) \notin l^1$, since its absolute value decays like n^{-1}, we do find $x(n) \in l^2$, because $|x(n)|^2$ is dominated by $(\pi n)^{-2}$, which does converge. If we let $\tilde{X}(\omega) = 1$ for $|\omega| \leq 1$ and $\tilde{X}(\omega) = 0$ otherwise, then

$$x(n) = \frac{1}{2\pi} \int_{-\pi}^{+\pi} \tilde{X}(\omega) \exp(j\omega n)\, d\omega \cdot \tag{7.65}$$

Thus, the IDTFT of $\tilde{X}(\omega)$ is $x(n)$. Figure 7.12 shows $\tilde{X}(\omega)$ and the discrete signal that results from its IDTFT.

Is $\tilde{X}(\omega)$ the DTFT of $x(n)$? Not exactly, but let us study the situation further. Since (7.65) is a Fourier series analysis equation, and $x(n)$ is a FS coefficient for $\tilde{X}(\omega)$, we can consider the limit of the corresponding Fourier series sum, $X(\omega)$. Then $X(\omega)$ converges for $\pm\omega = 1$ to $X(\omega) = 1/2$, the midpoint between the discontinuities:

$$\begin{aligned} X(\omega) &= \lim_{N \to \infty} \sum_{n=-N}^{n=+N} x(n) \exp(-j\omega n) \\ &= \sum_{n=-\infty}^{n=+\infty} x(n) \exp(-j\omega n) = \begin{cases} 1 & \text{if } |\omega| < 1, \\ 0 & \text{if } |\omega| > 1, \\ 1/2 & \text{if } |\omega| = 1. \end{cases} \end{aligned} \tag{7.66}$$

This is an unlucky result: for each $\omega \in [-\pi, \pi]$ the partial sums in (7.66) have a limit, but it is $X(\omega)$, not $\tilde{X}(\omega)$. The convergence of the partial sums in (7.66) is not uniform,

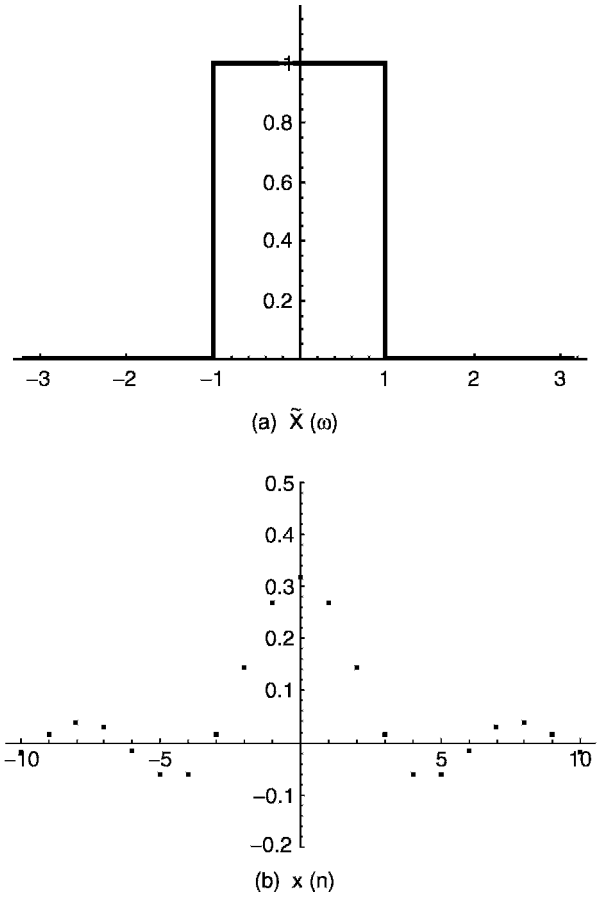

Fig. 7.12. Panel (a) shows a square pulse signal on $[-\pi, \pi]$. The result of applying the IDTFT to this pulse is shown in panel (b).

as it would be if $x(n)$ were absolutely summable. Instead, the convergence is in the $L^2[-\pi, \pi]$ norm, $\|\cdot\|_2$, and it allows the limit of the DTFT analysis equation, $X(\omega)$, to differ from the signal from which we derived $x(n)$ in the first place, $\tilde{X}(\omega)$.

Example (Gibbs Phenomenon). Examining the partial sums of (7.62) exposes a further feature of convergence under $\|\cdot\|_2$, namely the Gibbs[4] phenomenon. Spikes appear near the step edges in $\tilde{X}(\omega)$ and do not diminish with increasingly long partial sums (Figure 7.13).

[4]Josiah W Gibbs (1839–1903), an American chemist, physicist, and professor at yale University. Gibbs devised the vector dot product, $v \cdot w$, and the cross product, $v \times w$, and investigated the famous spike in Fourier series convergence. Although he was the first scientist of international stature from the United States, Yale neither appreciated his capabilities nor remunerated him for his service. Gibbs supported himself on an inheritance over the cource of a decade at Yale.

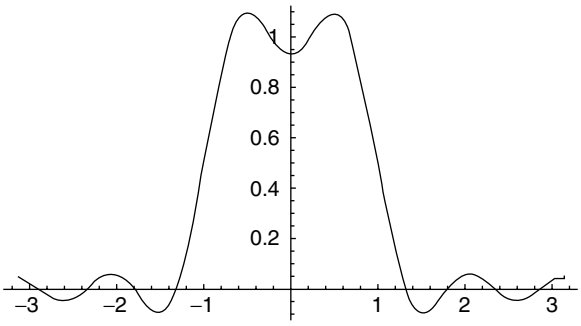

(a) Partial DTFT sum, $X_N(\omega)$, N = 5;

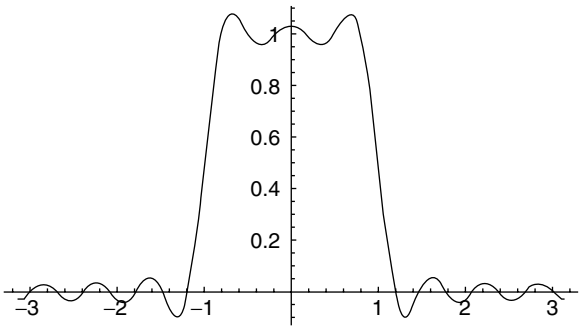

(b) $X_N(\omega)$, N = 10;

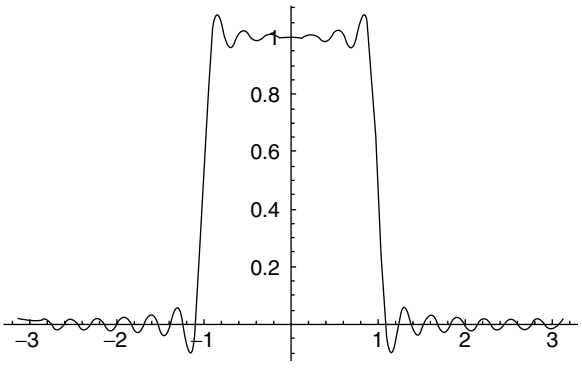

(c) $X_N(\omega)$, N = 20;

Fig. 7.13. A study of partial DTFT analysis equation sums for the square-summable signal $x(n) = \pi^{-1}\sin(n)$. Panel (a) shows $X_5(\omega)$; panel (b) shows $X_{10}(\omega)$; panel (c) shows $X_{20}(\omega)$; and panel (d), $X_{50}(\omega)$, shows a persistent ringing effect at the discontinuities.

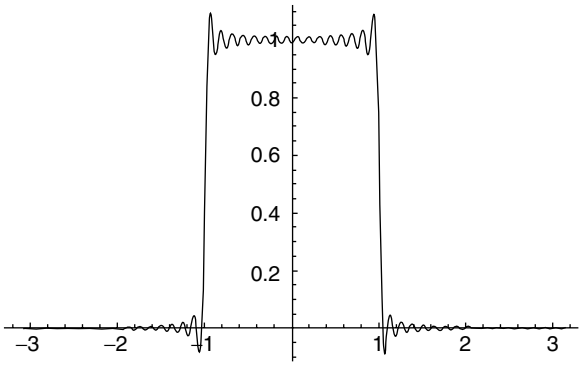

(d)

Fig. 7.13 (*Continued*)

Although its name has a supernatural resonance, there are specific, clearly definable reasons for the Gibbs phenomenon. In fact, it occurs whenever there is a discontinuity in a square integrable signal on $[-\pi, \pi]$. To more clearly grasp the reasons for the phenomenon, let us consider the partial DTFT sums, $X_N(\omega)$:

$$X_N(\omega) = \sum_{n=-N}^{n=+N} x(n)\exp(-j\omega n) = \sum_{n=-N}^{n=+N} \left\{ \frac{1}{2\pi} \int_{-\pi}^{+\pi} X(\Omega)\exp(j\Omega n)\ d\Omega \right\} \exp(-j\omega n)$$

$$= \frac{1}{2\pi} \sum_{n=-N}^{n=+N} \left\{ \int_{-\pi}^{+\pi} X(\Omega)\exp(j(\Omega-\omega)n)\ d\Omega \right\}. \tag{7.67}$$

The IDTFT of $X(\omega)$ replaces $x(n)$ in the finite summation of (7.67). $X(\omega)$ itself is the limit of these partial DTFT sums as $N \to \infty$. (We already know the definition of $X(\omega)$: It is the step function equal to unity on $[-1, 1]$ and zero elsewhere on $[-\pi, +\pi]$. It is thus possible to simplify the integral in (7.67), but we resist in order to show how the following development does not depend on the specific nature of $X(\omega)$.) Next, we set $\theta = \Omega - \omega$ toward a change of the integration variable, thereby giving

$$X_N(\omega) = \frac{1}{2\pi} \sum_{n=-N}^{n=+N} \left\{ \int_{-\pi-\omega}^{\pi-\omega} X(\theta+\omega)\exp(j\theta n)\ d\theta \right\}$$

$$= \frac{1}{2\pi} \sum_{n=-N}^{n=+N} \left\{ \int_{-\pi}^{\pi} X(\theta+\omega)\exp(j\theta n)\ d\theta \right\} \tag{7.68}$$

Note that the integrand is 2π-periodic, which permits us to take the limits of integration from $[-\pi, +\pi]$ instead of $[-\pi - \omega, \pi - \omega]$. Let us now interchange the finite summation and integration operations in (7.68) to obtain

$$X_N(\omega) = \int_{-\pi}^{\pi} X(\theta+\omega)\left\{\frac{1}{2\pi}\sum_{n=-N}^{n=+N}\exp(j\theta n)\right\}d\theta = \int_{-\pi}^{\pi} X(\theta+\omega)D_N(\theta)d\theta. \tag{7.69}$$

Therefore, the partial DTFT synthesis equation sums, $X_N(\omega)$, are given by the cross-correlation on $[-\pi, +\pi]$ of X and the Dirichlet[5] kernel of order N, $D_N(\theta)$. Chapter 5 introduced the Dirichlet kernel in connection with the problem of the Fourier series sum's convergence . It is an algebraic exercise to show that

$$D_N(\theta) = \frac{1}{2\pi}\sum_{n=-N}^{n=+N}\exp(j\theta n) = \frac{1}{2\pi}\frac{\sin\left(N\theta+\frac{\theta}{2}\right)}{\sin\left(\frac{\theta}{2}\right)} = \frac{1}{2\pi}+\frac{1}{\pi}\sum_{n=1}^{n=N}\cos(\theta n), \tag{7.70}$$

and therefore, for any $N > 0$,

$$\int_{0}^{\pi} D_N(\theta)\ d\theta = \frac{1}{2} = \int_{-\pi}^{0} D_N(\theta)\ d\theta\ . \tag{7.71}$$

Now, from (7.70) the Dirichlet kernel is an even function. So changing the variable of integration in (7.69) shows $X_N(\omega)$ to be a convolution of X and $D_N(\theta)$:

$$X_N(\omega) = \int_{-\pi}^{\pi} X(\theta+\omega)D_N(\theta)\ d\theta = \int_{-\pi}^{\pi} X(\theta)D_N(\omega-\theta)\ d\theta\ . \tag{7.72}$$

Now we understand the root cause of the Gibbs phenomenon. Because $X(\theta)$ in (7.72) is zero for $|\theta| > 1$, has discontinuities at $\theta = \pm 1$, and is unity for $|\theta| < 1$, the convolution integral produces a response that has a spike near the discontinuity. The spike's height is roughly the sum of the area of $D_N(\theta)$ under its main hump (Figure 7.14) plus the tail of the Dirichlet kernel that overlaps with the nonzero part of X.

The crux of the problem is how the first peak in the evaluation of the convolution integral behaves as $N \to \infty$. Empirically, as evidenced by Figure 7.13, the convolution generates a spike that shrinks in width but does not diminish in height. Clearly, the height of $D_N(\theta)$ does increase as $\theta \to 0$. Hence, it would appear that the area under the Dirichlet kernel between the first two zero crossings, $\pm\theta_N$, where $\theta_N = \pi/(N + 1/2)$, does not fall below some positive value. In fact, this area

[5]Peter Gustav Lejeune Dirichlet (1805–1859) studied convergence kernels for the Fourier series and problems in potential theory. He provided a proof of Fermat's Last Theorem for the case $n = 5$.

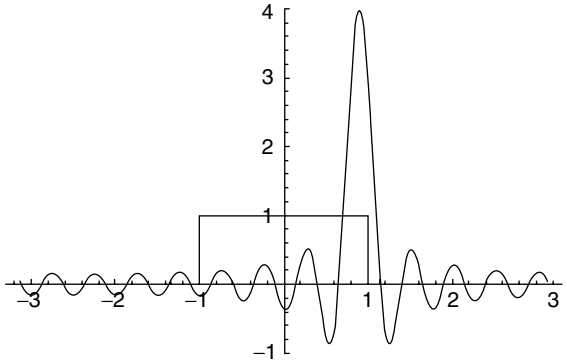

Fig. 7.14. Convolution with $D_N(\theta)$ at a discontinuity. A convolution integral of the analog signal X with the Dirichlet kernel of order N (here, $N = 12$) gives the partial DTFT summation for X, $X_N(\omega)$. The output is equal to the area under $D_N(\theta)$ that overlaps the nonzero area of the square pulse signal X.

remains constant! As $N \to \infty$, its decreasing width is perfectly balanced by the increasing height. Let us investigate:

$$\int_{-\theta_N}^{+\theta_N} D_N(\theta)\, d\theta = 2\int_{0}^{\theta_N} D_N(\theta)\, d\theta = \frac{1}{\pi}\int_{0}^{\theta_N} \frac{\sin\left(N\theta + \dfrac{\theta}{2}\right)}{\sin\left(\dfrac{\theta}{2}\right)}\, d\theta. \tag{7.73}$$

Making the change of integration variable $\Omega = N\theta + \theta/2$, we find

$$\int_{-\theta_N}^{+\theta_N} D_N(\theta)\, d\theta = \frac{1}{\pi}\int_{0}^{\pi} \frac{\sin(\Omega)}{\sin\left(\dfrac{\Omega}{2N+1}\right)} \frac{2}{2N+1}\, d\Omega = \frac{2}{\pi}\int_{0}^{\pi} \frac{\sin(\Omega)}{\Omega} \frac{\left(\dfrac{\Omega}{2N+1}\right)}{\sin\left(\dfrac{\Omega}{2N+1}\right)}\, d\Omega. \tag{7.74}$$

As $N \to \infty$, $\Omega/(2N + 1) \to 0$; taking the limit of (7.74) as $N \to \infty$ and interchanging the limit and integration operations on the right-hand side of (7.74) gives

$$\lim_{N\to\infty} \int_{-\theta_N}^{+\theta_N} D_N(\theta)\, d\theta = \frac{2}{\pi}\int_{0}^{\pi} \frac{\sin(\Omega)}{\Omega} \lim_{N\to\infty} \frac{\left(\dfrac{\Omega}{2N+1}\right)}{\sin\left(\dfrac{\Omega}{2N+1}\right)}\, d\Omega = \frac{2}{\pi}\int_{0}^{\pi} \frac{\sin(\Omega)}{\Omega}\, d\Omega \tag{7.75}$$

showing that the between the first zero crossings of $D_N(\theta)$ is constant. The area under $\text{sinc}(\Omega)$ from 0 to π is approximately 1.85194, so the convolution integral (7.72) for the partial DTFT summation, $X_N(\omega)$, evaluates to approximately

$(2/\pi)(1.85194) = 1.17898$. To find the approximate value of the convolution integral (7.72) at one of the Gibbs spikes, we must add the main hump's contribution to the area under the small oscillations in the tail of $D_N(\theta)$. What is this latter value? Figure. 7.14 shows the situation; these small osciallations overlap with the nonzero part of $X(\omega)$ and affect the convolution result. We know from (7.71) that the entire integral of $D_N(\theta)$ over $[-\pi, \pi]$ is unity. Thus, the integral over $[-1, 1]$ is also near unity, since (exercise) the areas of the oscillations decrease like $1/n$. So, we have

$$1 = \int_{-\theta_N}^{+\theta_N} D_N(\theta)\, d\theta + 2 \int_{+\theta_N}^{\pi} D_N(\theta)\, d\theta \approx 1.17898 + 2 \int_{+\theta_N}^{\pi} D_N(\theta)\, d\theta, \tag{7.76}$$

and therefore the maximum of the convolution, $X_N(\omega_{\max})$, approximates to

$$\begin{aligned} X_N(\omega_{\max}) &= \int_{-\pi}^{\pi} X(\theta) D_N(\omega_{\max} - \theta)\, d\theta \approx \int_{-\theta_N}^{+\theta_N} D_N(\theta)\, d\theta + \int_{+\theta_N}^{\pi} D_N(\theta)\ d\theta \\ &\approx 1.17898 - \frac{0.17898}{2} = 1.08949. \end{aligned} \tag{7.77}$$

A careful review of this analysis should convince the reader that

- Any step discontinuity in $X(\omega)$ will produce the same result.
- The amount of overshoot around the discontinuity is approximately 9% of the step height of the discontinuity.

The first point follows from the fact that for sufficiently high N values, the Dirichlet kernel's main peak will be so narrow that $X(\omega)$ will appear flat before and after the jump. That is, $D_N(\theta)$ localizes the discontinuity of $X(\omega)$. The second point is perhaps easier to witness from the present example. The size of the Gibbs phenomenon's spike is given by an integral, which is a linear operation, and so scaling the step height causes the convolution's output to scale accordingly. The rich Fourier analysis literature provides further explanations and generalizations of the Gibbs phenomenon [15–17].

7.2.1.5 Some Final Points. This section concludes our preliminary study of the DTFT by stating two theoretical results.

Not all of our abstract l^p signal spaces support a DTFT; however, we have the following result [18]:

Theorem (DTFT Existence for *p*-Summable Signals). Suppose $x(n) \in l^p$, for $1 < p < 2$. Then there exists an $X(\omega) \in L^q[-\pi, \pi]$, where p and q are conjugate exponents (that is, $p^{-1} + q^{-1} = 1$), such that the values $x(n)$ are the Fourier series coefficients for $X(\omega)$.

Thus, we have a rich variety of signal spaces whose members have DTFTs. In signal analysis, the limiting cases—l^1 and l^2—are the most important. For $x(n) \in l^1$, the partial sums, $X_N(\omega)$, converge uniformly on $[-\pi, \pi]$ to a continuous signal, $X(\omega)$. Because $X(\omega)$ is continuous on a closed interval, $[-\pi, \pi]$, it is also bounded: $X(\omega) \in L^\infty$. The partial DTFT sums, $X_N(\omega)$, converge pointwise when $x(n)$ is absolutely summable. This is not the case for square-summable signals; we have seen that pointwise convergence does not necessarily occur for $x(n) \in l^2$. A long-standing problem has been to characterize the set of points for which the Fourier series of an $L^2[-\pi, \pi]$ signal converges. Many mathematicians supposed that convergence occurs almost everywhere, and in 1966 Carleson finally proved [19] the following theorem:

Theorem (Carleson's). If $X(\omega) \in L^2[-\pi, \pi]$, then the Fourier series for X converges almost everywhere to $X(\omega)$.

This result was soon generalized by Hunt to any $L^p[-\pi, \pi]$, $1 < p < \infty$ [20]. The exceptional case is $L^1[-\pi, \pi]$. And what a exception it is: In 1926, Kolmogorov[6] found an unbounded, discontinuous function, $f \in L^1[-\pi, \pi]$, whose Fourier series diverges everywhere from f [21, 22].

7.2.2 Properties

Let us enumerate the properties of the discrete-time Fourier transform. We assume throughout that discrete signals, say $x(n)$, belong to some signal space that supports a DTFT operation. Many of these are similar in flavor to the properties of previously covered transforms: the Fourier series, Fourier transform, and discrete Fourier transform. Consequently, we leave several of the proofs as exercises.

Proposition (Linearity, Time-Shift, and Frequency Shift). Let $x(n)$ and $y(n)$ be discrete signals and let $X(\omega)$ and $Y(\omega)$ be their DTFTs, respectively. Then

(a) (Linearity) The DTFT of $ax(n) + by(n)$ is $aX(\omega) + bY(\omega)$.
(b) (Time Shift) The DTFT of $x(n - m)$ is $\exp(-j\omega m)X(\omega)$.
(c) (Frequency Shift) The IDTFT of $X(\omega - \theta)$ is $\exp(-j\theta n)x(n)$.

Proof: Exercise. ■

[6]A. N. Kolmogorov (1903–1987), professor of mathematics at Moscow State University, investigated problems of topology and analysis and established the axiomatic approach to probability theory.

Proposition (Frequency Differentiation). Suppose $x(n)$ is a discrete signal, $X(\omega)$ is its DTFT, and the partial sums $X_N(\omega)$ converge uniformly on $[-\pi, \pi]$ to $X(\omega)$. Then the DTFT of $nx(n)$ is $jdX(\omega)/d\omega$.

Proof: To prove transform properties, one may work from either end of a proposed equality; in this case, it is easier to manipulate the derivative of the DTFT. To wit,

$$j\frac{d}{d\omega}X(\omega) = j\frac{d}{d\omega}\sum_{n=-\infty}^{\infty} x(n)\exp(-jn\omega) = j\sum_{n=-\infty}^{\infty} x(n)\frac{d}{d\omega}\exp(-jn\omega). \tag{7.78}$$

The interchange of the differentiation and infinite summation operations is valid because the DTFT analysis equation is uniformly convergent. Taking the derivative of the summand in (7.78) and pulling the constants through the summation gives

$$j\frac{d}{d\omega}X(\omega) = j\sum_{n=-\infty}^{\infty} x(n)(-jn)\exp(-jn\omega) = \sum_{n=-\infty}^{\infty} nx(n)\exp(-jn\omega). \tag{7.79}$$

This is precisely the DTFT analysis equation for the signal $nx(n)$. ■

Without a doubt, the most important property of the DTFT is the Convolution-in-Time Theorem. This result shows that convolving two signals in the time domain is equivalent to multiplying their frequency domain representations. Since we are dealing with aperiodic signals, there is no need to redefine convolution for a finite interval, as we did with the DFT in (7.22). The convolution-in-time property is the key to understanding signal filtering—the selective suppression of frequency bands within a signal. We shall resort to this theorem many times in the chapters that follow.

Theorem (Convolution in Time). Let $x(n)$ and $y(n)$ be signals, let $X(\omega)$ and $Y(\omega)$ be their DTFTs, and let $z = x * y$. If the convolution sum for $z(n)$ converges absolutely for each integer n, then the DTFT of $z(n)$ is $Z(\omega) = X(\omega)Y(\omega)$.

Proof: Among all of the theoretical investigations into all of the transforms studied so far, we should note a distinct computational compatibility between the transform integral (or summation) and the convolution operation. The DTFT is no exception. We substitute the expression for the convolution, $z = x * y$, directly into the DTFT analysis equation for $Z(\omega)$:

$$
\begin{aligned}
Z(\omega) &= \sum_{n=-\infty}^{\infty} z(n)\exp(-j\omega n) = \sum_{n=-\infty}^{\infty} (x*y)(n)\exp(-j\omega n) \\
&= \sum_{n=-\infty}^{\infty} \left(\sum_{k=-\infty}^{\infty} x(k)y(n-k) \right) \exp(-j\omega n) \\
&= \sum_{n=-\infty}^{\infty} \sum_{k=-\infty}^{\infty} x(k)y(n-k)\exp(-j\omega\,(n-k))\exp(-j\omega k) \\
&= \sum_{k=-\infty}^{\infty} \sum_{n=-\infty}^{\infty} x(k)y(n-k)\exp(-j\omega\,(n-k))\exp(-j\omega k) \\
&= \sum_{k=-\infty}^{\infty} x(k)\exp(-j\omega k) \sum_{n=-\infty}^{\infty} y(n-k)\exp(-j\omega\,(n-k)) \\
&= X(\omega) \sum_{n=-\infty}^{\infty} y(n-k)\exp(-j\omega\,(n-k)) \\
&= X(\omega) \sum_{m=-\infty}^{\infty} y(m)\exp(-j\omega m) = X(\omega)Y(\omega). \qquad (7.80)
\end{aligned}
$$

We use the absolute convergence of the convolution sum to justify writing the iterated summation as a double summation and to subsequently switch the order to the summation. A routine change of summation variable, $m = n - k$, occurs in the last line of (7.80). ■

There is an important link back to our results on linear, translation-invariant systems. Recall from Chapter 2 that the convolution relation characterizes LTI systems. If H is LTI, then the output, $y = Hx$, is the convolution of $h = H\delta$ with x: $y = h * x$. Thus we have the following corollary.

Corollary (Convolution in Time). If H is an LTI system, h is the impulse response of H, and $y = Hx$, then $Y(\omega) = X(\omega)H(\omega)$, assuming their DTFTs exist.

Proof: Note that $y = h * x$ and apply the theorem. ■

We shall establish yet another transform Convolution Theorem when we study the z-transform in Chapter 8. The next theorem is a companion result. It establishes for the DTFT a familiar link: Multiplication in the time domain equates with convolution in the frequency domain. This theorem has a z-transform variant, too.

Theorem (Convolution in Frequency). Suppose $x(n)$ and $y(n)$ are discrete signals; $X(\omega)$, $Y(\omega) \in L^2[-\pi, \pi]$ are their respective DTFTs; and $z(n) = x(n)y(n)$ is their

termwise product. Then the DTFT of $z(n)$, $Z(\omega)$, is given by the scaled convolution of $X(\omega)$ and $Y(\omega)$ in $L^2[-\pi, \pi]$:

$$Z(\omega) = \frac{1}{2\pi} \int_{-\pi}^{+\pi} X(\theta) Y(\omega - \theta)\, d\theta. \tag{7.81}$$

Proof: The right-hand side of (7.81) is the integral of the product of infinite summations whose terms contain the complex exponential—for instance, $\exp(-j\theta n)$. We have already witnessed numerous cases where the summands cancel owing to the 2π-periodicity of the exponential. Therefore, let us work from the $L^2[-\pi, \pi]$ side of (7.81). Indeed, we compute,

$$\begin{aligned}
\frac{1}{2\pi} \int_{-\pi}^{+\pi} X(\theta) Y(\omega - \theta)\, d\theta &= \frac{1}{2\pi} \int_{-\pi}^{+\pi} \sum_{n=-\infty}^{\infty} x(n) \exp(-j\theta n) \sum_{k=-\infty}^{\infty} y(k) \exp[-j(\omega - \theta)k]\ d\theta \\
&= \frac{1}{2\pi} \sum_{n=-\infty}^{\infty} \sum_{k=-\infty}^{\infty} x(n) y(k) \exp(-j\omega k) \int_{-\pi}^{+\pi} \exp(-j\theta n) \exp(j\theta k)\, d\theta \\
&= \frac{1}{2\pi} \sum_{n=-\infty}^{\infty} \sum_{k=-\infty}^{\infty} x(n) y(k) \exp(-j\omega k) \int_{-\pi}^{+\pi} \exp[-j\theta(n-k)]\ d\theta.
\end{aligned} \tag{7.82}$$

Once again the last integral is zero, unless $n = k$; in this case it evaluates to 2π. Thus, all of the terms of the double summation on the bottom of (7.82) are zero, save those where $n = k$. Our strategy works, and we find

$$\begin{aligned}
\frac{1}{2\pi} \int_{-\pi}^{+\pi} X(\theta) Y(\omega - \theta)\, d\theta &= \frac{1}{2\pi} \sum_{n=-\infty}^{\infty} \sum_{k=-\infty}^{\infty} x(n) y(k) \exp(-j\omega k) \int_{-\pi}^{+\pi} \exp[-j\theta(n-k)]\, d\theta \\
&= \frac{2\pi}{2\pi} \sum_{n=-\infty}^{\infty} x(n) y(n) \exp(-j\omega n) = \sum_{n=-\infty}^{\infty} z(n) \exp(-j\omega n) = Z(\omega)
\end{aligned} \tag{7.83}$$

which completes the proof. ■

Note that the above proof allows for the case that the signal $y(n)$ may be complex-valued. This observation gives us the following corollary.

Corollary. Again let $x(n)$ and $y(n)$ be discrete signals, and let $X(\omega), Y(\omega) \in L^2[-\pi, \pi]$ be their respective DTFTs. Then,

$$\sum_{n=-\infty}^{\infty} x(n) \overline{y}(n) = \frac{1}{2\pi} \int_{-\pi}^{+\pi} X(\theta) \overline{Y}(\theta)\, d\theta. \tag{7.84}$$

Proof: Before commencing with the proof, let us observe that the left-hand side of (7.84) is the l^2 inner product of $x(n)$ and $y(n)$, and the right-hand side is just the inner product of $X(\omega)$ and $Y(\omega)$ scaled by the factor $(2\pi)^{-1}$. Well, in the course of establishing the embedding isomorphism from l^2 into $L^2[-\pi, \pi]$ as Hilbert spaces, we already proved this result. Nonetheless, we can convey some of the symmetry properties and computational mechanics of the DTFT by offering another argument. So set $w(n) = \overline{y}\,(n)$ and $z(n) = x(n)w(n) = x(n)\overline{y}\,(n)$. By the theorem, then, the DTFT of $z(n)$ is

$$Z(\omega) = \frac{1}{2\pi} \int_{-\pi}^{+\pi} X(\theta)W(\omega - \theta)\, d\theta. \tag{7.85}$$

Therefore,

$$Z(0) = \left(\sum_{n=-\infty}^{+\infty} z(n)e(-j\omega n) \right)\Bigg|_{\omega=0} = \sum_{n=-\infty}^{+\infty} x(n)\overline{y}(n) = \frac{1}{2\pi} \int_{-\pi}^{+\pi} X(\theta)W(-\theta)\, d\theta. \tag{7.86}$$

What is $W(-\theta)$ in the integral on the right-hand side of (7.86)? By the algebra of complex conjugates, however, we find

$$\overline{Y}(\theta) = \overline{\left[\sum_{n=-\infty}^{+\infty} y(n)e(-j\theta n) \right]} = \sum_{n=-\infty}^{+\infty} \overline{y}(n)e(j\theta n) = \sum_{n=-\infty}^{+\infty} \overline{y}(n)e[-j(-\theta)n] = W(-\theta). \tag{7.87}$$

Putting (7.86) and (7.87) together establishes the theorem's result. ■

Corollary (Parseval's Theorem). If $x(n) \in l^2$, then $\|x(n)\|_2 = (2\pi)^{-1}\|X(\omega)\|_2$.

Proof: Take $x(n) = y(n)$ in the previous corollary. (Observe that the two norms in the statement of Parseval's theorem are taken in two different Hilbert spaces: l^2 and $L^2[-\pi, \pi]$.) ■

Note that Parseval's theorem too follows from our earlier Hilbert space isomorphism. Many frequency transform theorems at first glance appear to be almost miraculous consequences of the properties of the exponential function, or its sinusoidal parts, or the definition of the particular discrete or analog transform. But in fact they are mere instances of Hilbert space results. That very general, very abstract, partly algebraic, partly geometric theory that we studied in Chapters 2 and 3 provides us with many of the basic tools for the frequency domain processing and analysis of signals.

Parseval's theorem shows that signal energy in the time domain is proportional to signal energy in the frequency domain. This has some practical applications. In Chapter 9 we shall consider frequency-domain analysis of signals. We sought methods for discovering the periodicities of signals in Chapter 4, and to some extent we were

successful in applying statistical and structural methods toward this end. Using discrete Fourier transforms, such as the DFT or the DTFT, we can obtain a description of the signal in terms of its frequency content. Then, in order to decide whether one or another frequency is present in the time-domain signal, we examine the frequency-domain representation for significant values at certain frequencies. But what constitutes a significant value? We can threshold signals in the frequency domain, just as we did in the time domain in Chapter 4. But, again, how do we set the threshold for what constitutes a significant frequency component? Parseval's theorem tells us that we can look for a sufficient portion of the signal's energy within a frequency range. We know that the overall frequency-domain energy is proportional to the overall time-domain energy, and the time-domain energy is computable from the signal values. Thus, we can select a threshold for the frequency domain based on some percentage of time-domain energy. Since we know that the total frequency domain energy is proportional to time-domain energy, we do not even have to examine other bands once the threshold is exceeded in some range of frequencies.

As with the DFT, there are a variety of DTFT symmetry properties. At this stage in our exposition, these are routine, and we leave them as exercises. The next section covers a property of the DTFT that applies to linear, translation-invariant systems. It turns out that with the DTFT, we can show that LTI systems have a very benign effect on exponential signals.

7.2.3 LTI Systems and the DTFT

Let us return to the idea of a discrete, linear, translation-invariant system. We introduced discrete LTI systems in the second chapter, and there we showed that LTI systems are characterized by the convolution relation. The system output, $y = Hx$, is the convolution of the input with a fixed signal, $y = h * x$, where $h = H\delta$. The discrete signal $h(n)$ is called the impulse response of the LTI system H. There is a close, important relationship between LTI systems and the DTFT.

Recall that an eigenvector for a finite-dimensional linear map, T, is a vector $\boldsymbol{v}$ for which $\boldsymbol{Tv} = \boldsymbol{av}$, for some constant a. Similarly, we can define an eigenfunction for a system, to be a signal for which $y = Hx = ax$, for some constant value a.

Theorem (Eigenfunctions of LTI Systems). If H is an LTI system, $y = Hx$, where $x(n) = \exp(j\omega n)$, then $x(n)$ is an eigenfunction of the system H.

Proof: By the Convolution Theorem for LTI systems, we have

$$y(n) = (h * x)(n) = \sum_{k=-\infty}^{+\infty} h(k)x(n-k) = \sum_{k=-\infty}^{+\infty} h(k)\exp[j\omega(n-k)]$$

$$= \exp(j\omega n) \sum_{n=-\infty}^{+\infty} h(k)\exp(-j\omega k) = \exp(j\omega n)H(\omega), \tag{7.88}$$

where $H(\omega)$ is the DTFT of $h(n)$. ■

The theorem inspires the following definition.

Definition (Frequency Response of LTI Systems). If H is an LTI system, and $h = H\delta$, is the impulse response of H, then $H(\omega)$, the DTFT of $h(n)$, is called the *frequency response* of H.

Note that we have a notational conflict, in that we are using the uppercase H to denote both the LTI system and its frequency response. Of course, writing the frequency response as a function of ω helps to distinguish the two. The context usually makes clear which is the system and which is the frequency-domain representation of the impulse response. So we persist in using the notation, which is a widespread signal theory convention.

It is the behavior of $H(\omega)$ as a function of ω that determines how an LTI system, H, affects the frequencies within a discrete signal. The Eigenfunctions Theorem showed that if $x(n) = \exp(j\omega n)$ is an exponential signal, and $y = Hx$, then $y(n) = x(n)H(\omega)$. So the magnitude of the output, $|y(n)|$, is proportional to the magnitude of the input, $|x(n)|$, and the constant of proportionality is $|H(\omega)|$. Thus, if $|H(\omega)|$ is small, then the system suppresses exponential signals of radial frequency w. And if $|H(\omega)|$ is large, then H passes exponentials $\exp(j\omega n)$. What is meant, however, by the "frequencies within a discrete signal?" If the input signal consists of a pure exponential, $x(n) = \exp(j\omega n) = \cos(\omega n) + j\sin(\omega n)$, of frequency ω radians/second, then the frequency component within the signal is the exponential. It consists of a real and an imaginary sinusoidal component. And, by the theorem, the system's frequency response determines how the system affects the frequency components of $x(n)$. Furthermore, suppose the input signal consists of a sum of scaled exponentials,

$$x(n) = \sum_{k=M}^{N} c_k \exp(j\omega_k n). \tag{7.89}$$

By linearity we have

$$\begin{aligned} y(n) = H[x(n)] &= H\left[\sum_{k=M}^{N} c_k \exp(j\omega_k n)\right] = \sum_{k=M}^{N} c_k H\left[\exp(j\omega_k n)\right] \\ &= \sum_{k=M}^{N} c_k H\left[\exp(j\omega_k n)\right] = \sum_{k=M}^{N} c_k \exp(j\omega_k n) H(\omega_k) = \sum_{k=M}^{N} H(\omega_k) c_k \exp(j\omega_k n). \end{aligned} \tag{7.90}$$

Thus, the output consists of the sum of $x(n)$'s frequency components, each further attenuated or amplified by its corresponding value, $H(\omega_k)$. But is it still correct to refer to a general signal's frequency components?

Within certain classes of aperiodic signals, it is indeed possible to approximate them arbitrarily well with sums of exponentials, such as in (7.89). If we can show this, then this justifies the above characterization of the frequency response as admitting and suppressing the various frequency components within a signal (7.90). Let us state our desired result as a theorem.

Theorem (Frequency Components of Aperiodic Signals). Let the signal $x(n)$ have DTFT $X(\omega)$. If $x(n)$ is absolutely summable or square-summable, then it can be approximated arbitrarily well by linear combinations of exponential signals of the form $\{\exp(jn\omega) : \omega = \pi(2m - M)/M$ for some m, $0 < m < M - 1$, $1 < M\}$.

Proof: The key idea is to approximate the synthesis equation integral representation for $x(n)$ in terms of $X(\omega)$:

$$x(n) = \frac{1}{2\pi}\int_{-\pi}^{+\pi} X(\omega)\exp(j\omega n)\, d\omega. \tag{7.91}$$

The trapezoidal rule approximates $x(n)$ by dividing the interval $[-\pi, \pi]$ into $N > 0$ segments of equal width, $2\pi/N$, and summing the areas of the trapezoidal regions. Let $y(n, \omega) = X(\omega)\exp(j\omega n)$. Then, $y(n, -\pi) = y(n, \pi)$, and after some simplification, we get

$$\begin{aligned} x(n) &\approx \frac{1}{M}\left[y(n,-\pi) + y(n,-\pi+2\pi/M) + y(n,-\pi+4\pi/M) + \cdots + y(n,\pi-2\pi/M)\right] \\ &= \frac{1}{M}\sum_{m=0}^{M-1} y(n,-\pi+2\pi m/M) = \frac{1}{M}\sum_{m=0}^{M-1} X(-\pi+2\pi m/M)\exp[jn(-\pi+2\pi m/M)] \\ &= \frac{1}{M}\sum_{m=0}^{M-1} X(-\pi+2\pi m/M)\exp\left[jn\pi\left(\frac{2m-M}{M}\right)\right]. \end{aligned} \tag{7.92}$$

Since (7.92) is a linear combination of terms of the form $A_m\exp(jn\omega)$, where A_m is a constant, and $\omega = \pi(2m - M)/M$, the proof is complete. ■

Now, it is possible to investigate the effect an LTI system H, where $h = H\delta$, has on an aperiodic input signal $x(n)$. We first closely approximate $x(n)$ by a linear combination of exponential terms, $\exp(jn\omega)$, $\omega = \pi(2m - M)/M$, as given by the Frequency Components Theorem. By the Eigenfunctions Theorem, the various component exponential terms scale according to the value of the DTFT of $h(n)$, $H(\omega)$:

$$\begin{aligned} y(n) = (h * x)(n) &= \left(h * \sum_{m=0}^{M-1} A_m \exp\left[jn\frac{\pi(2m-M)}{M}\right]\right)(n) \\ &= \sum_{m=0}^{M-1} A_m \exp\left[jn\frac{\pi(2m-M)}{M}\right] H\left(\frac{\pi(2m-M)}{M}\right) = \sum_{m=0}^{M-1} A_m \exp(jn\omega_m) H(\omega_m). \end{aligned} \tag{7.93}$$

Depending on the value of $H(\omega_m)$ at various values of ω_m, then, the frequency components of $x(n)$ are attenuated or amplified by the LTI system H.

Example (Perfect High-Frequency Attenuation System). Let us explore a system H that removes all frequency components above a certain fixed radial frequency, ω_c, from a discrete aperiodic signal, $x(n)$. There is a practical need for such systems. They remove noise from signals prior to segmentation and classification, as we noted in Chapter 4. If the time-domain filter $h(n)$ removes all frequency components above ω_c, the DTFT of $h(n)$, $H(\omega)$, must be zero for $|\omega| > |\omega_c|$, as Figure 7.15 shows. We can compute $h(n)$ for the square pulse in Fig. 7.15(a) as follows.

$$h(n) = \frac{1}{2\pi}\int_{-\pi}^{+\pi} X(\omega) exp(jn\omega)\, d\omega = \frac{1}{2\pi}\int_{-\omega_c}^{+\omega_c} \exp(jn\omega)\, d\omega$$
$$= \frac{1}{2\pi}\frac{\exp(jn\omega)}{jn}\Bigg|_{-\omega_c}^{+\omega_c} = \frac{\sin(n\omega_c)}{\pi n} = \frac{\omega_c}{\pi}\text{sinc}(n\omega_c). \tag{7.94}$$

However flawless it may be in the frequency domain, as a time-domain noise removal filter, $h(n)$ is quite imperfect. Two fundamental problems render it physically impossible to implement:

- It has infinite support.
- The system H is non causal: $h(n) = 0$ for $n < 0$.

The first point means that we can never finish the convolution sum necessary to calculate the output $y = Hx$. Of course, we can come very close to approximating the

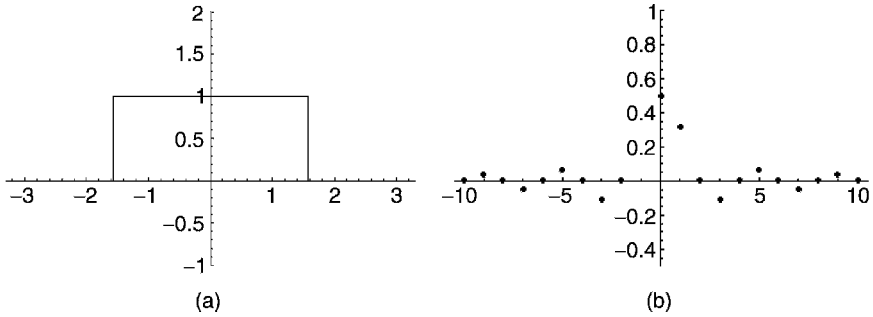

Fig. 7.15. Perfect high-frequency removal. The system with impulse response $h(n)$ and DTFT $H(\omega)$ will remove all frequencies above ω_c if $H(\omega) = 0$ for $|\omega| > \omega_c$. We also expect that H will perfectly preserve frequencies within the range $[-\omega_c, \omega_c]$; in other words, if $|\omega| \leq \omega_c$, then $H(\omega) = 1$. Thus, $H(\omega)$ resembles a square pulse centered in $[-\pi, \pi]$, as in panel (a). Here, $\omega_c = \pi/2$. The time-domain sinc signal in (b) gives rise to such a frequency-domain representation.

perfect filter output by prolonging the summation until further terms are negligible. But worse is the non causality. This implies that computing the convolution $y = h * x$ requires future values of the input signal $x(n)$. In the next chapter we shall uncover filter design techniques that avoid these problems.

7.3 THE SAMPLING THEOREM

Presentations of signal theory throughout the text have alternated between analog developments and discrete developments. We have worked either in the analog world or in the discrete world. Sampling an analog signal at regular intervals produces a discrete signal, but so far nothing has been proffered as an interconnection between the analog source and the discrete result. However, now have the theoretical tools in hand to effect a unification of the two realms of signal theory. The unification takes place using not time domain methods, but rather frequency-domain methods. Perhaps this is not so unexpected. After all, we noted that the discrete-time Fourier transform very much resembles the analog Fourier series and that there is a Hilbert space isomorphism between the analog space $L^2[-\pi, \pi]$ (or, more precisely, its equivalence classes of signals equal almost everywhere) and the discrete space l^2.

7.3.1 Band-Limited Signals

One of the key ideas in linking the analog and discrete worlds is the notion of a bandlimited analog signal. This means, informally, that the frequency-domain representation of the signal has finite support. Physically, this is a realistic assumption, as no physical signal can have frequency components that go arbitrarily high in frequency. Nature can only shake so fast.

Definition (Band-Limited Signal). An analog signal $x(t)$ is *band-limited* if its Fourier transform, $X(\omega)$, exists and has finite support.

To discover the connection to band-limited signals, let us consider anew the operation of sampling an analog signal. If $x(t)$ is a continuous, absolutely integrable analog signal and $T > 0$, then it may be sampled at intervals T to produce the discrete signal $s(n) = x(nT)$. Let us suppose that $s(n) \in l^1$ so that the DTFT sum converges uniformly to $S(\omega)$,

$$S(\omega) = \sum_{n=-\infty}^{+\infty} s(n) \exp(-jn\omega), \tag{7.95}$$

and, hence, that $s(n)$ is represented by the DTFT synthesis equation,

$$s(n) = \frac{1}{2\pi} \int_{-\pi}^{+\pi} S(\omega) \exp(j\omega n)\, d\omega \tag{7.96}$$

Because $x(t) \in L^1$, $x(t)$ is represented by the FT's synthesis equation,

$$x(t) = \frac{1}{2\pi} \int_{-\infty}^{+\infty} X(\omega) \exp(j\omega t)\, d\omega \tag{7.97}$$

where $X(\omega)$ is the radial Fourier transform of $x(t)$. Since $s(n) = x(nT)$, we get another representation of $s(n)$:

$$s(n) = x(nT) = \frac{1}{2\pi} \int_{-\infty}^{+\infty} X(\omega) \exp(j\omega nT)\, d\omega \tag{7.98}$$

Now we have a derivation of the discrete signal values from both a discrete frequency representation (7.96) and from an analog frequency representation (7.98). The observation is both easy and important. (The reason that we did not take note of this earlier is that only now do we have Fourier and inverse Fourier transforms for both analog and discrete signals!) The key to discovering the hidden bond between the analog and discrete signal domains lies in finding mathematical similarities in the integrands of the DTFT and FT synthesis equations.

Connecting the two integrands in (7.96) and (7.98) involves both the sampling interval, T, and the bandwidth of the original analog signal, $x(t)$. Since the IFT integral (7.98) has infinite limits, and the IDTFT integral has finite limits, the prospects for relating the two integrands seem dim. Note, however, that if the FT of $x(t)$ is band-limited, then the nonzero values of $X(\omega)$ are confined to an interval, $[-b, +b]$, where $b > 0$. The FT integral representation of $s(n)$ becomes

$$s(n) = x(nT) = \frac{1}{2\pi} \int_{-b}^{+b} X(\omega) \exp(j\omega nT)\, d\omega \tag{7.99}$$

A change of integration variable, $\theta = \omega T$, converts (7.99) into the form

$$s(n) = x(nT) = \frac{1}{2\pi T} \int_{-bT}^{+bT} X\left(\frac{\theta}{T}\right) \exp[jn\theta]\, d\theta \tag{7.100}$$

Now, if the interval $[-bT, bT] \subseteq [-\pi, \pi]$, then the integrals (7.96) and (7.100) are comparable. Suppose we choose T small enough so that this is true; we space the discrete samples of $x(t)$ so close together that $bT < \pi$. Since $X(\theta/T)$ is zero outside $[-bT, bT]$,

$$s(n) = x(nT) = \frac{1}{2\pi} \int_{-\pi}^{+\pi} \frac{1}{T} X\left(\frac{\theta}{T}\right) \exp[jn\theta]\, d\theta \tag{7.101}$$

(Observe carefully that none of this analysis would be valid without $x(t)$ being band-limited.) Now there are two different representations of the discrete signal $x(n)$: one (7.96) dependent on $S(\omega)$, the DTFT of $s(n)$, and another (7.101) dependent on a

scaled, amplified portion of the FT of $x(t)$: $T^{-1}X(\theta/T)$. We know that the DTFT is unique, since it is invertible, and therefore we have $S(\omega) = T^{-1}X(\omega/T)$.

Let us summarize. If the analog signal, $x(t)$, is band-limited, then a sufficiently high sampling rate, T, guarantees that the DTFT of $s(n) = x(nT)$ and the (scaled, amplified) FT of $x(t)$ are equal.

In principle, this fact allows us to reconstruct $x(t)$ from its discrete samples. Suppose, again, that $s(n) = x(nT)$ and that T is so small that $bT < \pi$, where $X(\omega)$ is zero outside $[-b, b]$. From the samples, $s(n)$, we compute the DTFT, $S(\omega)$. Now, by the preceding considerations, $S(\omega) = T^{-1}X(\omega/T)$; in other words, $TS(\omega T) = X(\omega)$. Now we can compute $x(t)$ as the IFT of $X(\omega)$. So, indeed, the samples of a band-limited analog signal can be chosen close enough together that the original signal can be recovered from the samples.

The next section we will give this abstract observation some practical value.

7.3.2 Recovering Analog Signals from Their Samples

Now let us work toward a precise characterization of the conditions under which an analog signal is recoverable by discrete samples. One outcome of this will be an elucidation of the concept of aliasing, which occurs when the conditions for ideal reconstruction are not completely met.

In the previous section we studied the relationship between the DTFT and the FT for band-limited signals $x(t)$ and discrete signals $s(n) = x(nT)$, $T > 0$. The next theorem relaxes the assumption that $x(t)$ is band-limited.

Theorem (DTFT and FT). Suppose that $x(t) \in L^1$ is an analog signal, $T > 0$, and $s(n) = x(nT)$. If $s(n) \in l^1$ so that the DTFT sum converges uniformly to $S(\omega)$, then

$$S(\omega) = \frac{1}{T}\sum_{k=-\infty}^{+\infty} X\left(\frac{\omega + 2\pi k}{T}\right). \tag{7.102}$$

Proof: Continuing the development of the previous section, we set $\theta = \omega T$ for a change of integration variable:

$$s(n) = x(nT) = \frac{1}{2\pi}\int_{-\infty}^{+\infty} X(\omega)\exp(j\omega nT)\, d\omega = \frac{1}{2\pi T}\int_{-\infty}^{+\infty} X\left(\frac{\theta}{T}\right)\exp(j\theta n)\, d\theta. \tag{7.103}$$

Let $Y(\theta) = T^{-1}X(\theta/T)$. Then,

$$s(n) = x(nT) = \frac{1}{2\pi}\int_{-\infty}^{+\infty} X(\omega)\exp(j\omega nT)\, d\omega = \frac{1}{2\pi}\int_{-\infty}^{+\infty} Y(\theta)\exp(j\theta n)\, d\theta. \tag{7.104}$$

If we assume that $x(t)$ is band-limited, then X—and hence Y—have finite support; this reduces (7.104) to a finite integral as in the previous section. Let us not assume here that $x(t)$ is band-limited and instead investigate how (7.104) can be written as a

sum of finite integrals. Indeed, we can break (7.104) up into 2π-wide chunks as follows:

$$s(n) = \frac{1}{2\pi}\int_{-\infty}^{+\infty} Y(\theta)\exp(j\theta n)\,d\theta = \frac{1}{2\pi}\sum_{k=-\infty}^{\infty}\int_{-\pi+2\pi k}^{\pi+2\pi k} Y(\theta)\exp(j\theta n)\,d\theta \tag{7.105}$$

The insight behind this is that the chunk of $Y(\theta)$ corresponding to $k = 0$ should look like $S(\omega)$ on $[-\pi, \pi]$, and the others, corresponding to $k = 0$, should be negligible if T is small and $x(t)$ is approximately band-limited. Now set $\phi = \theta - 2\pi k$ to get

$$\begin{aligned} s(n) &= \frac{1}{2\pi}\sum_{k=-\infty}^{\infty}\int_{-\pi}^{\pi} Y(\phi+2\pi k)\exp[j(\phi+2\pi k)n]\,d\phi \\ &= \frac{1}{2\pi}\sum_{k=-\infty}^{\infty}\int_{-\pi}^{\pi} Y(\phi+2\pi k)\exp(j\phi n)\,d\phi = \frac{1}{2\pi}\int_{-\pi}^{\pi}\sum_{k=-\infty}^{\infty} Y(\phi+2\pi k)\exp(j\phi n)\,d\phi \end{aligned} \tag{7.106}$$

The interchange of the order of the summation and the integration is allowable, because the sum converges uniformly to $Y(\theta)$ on $\mathbb{R}$. Now we have (7.106) in the form of the DTFT synthesis equation (7.96) for $s(n)$:

$$s(n) = \frac{1}{2\pi}\int_{-\pi}^{\pi} S(\omega)\exp(j\omega n)\,d\omega = \frac{1}{2\pi}\int_{-\pi}^{\pi}\sum_{k=-\infty}^{\infty} Y(\omega+2\pi k)\exp(j\omega n)\,d\omega \tag{7.107}$$

Since the DTFT is invertible, together (7.107) entails

$$S(\omega) = \sum_{k=-\infty}^{\infty} Y(\omega+2\pi k) = \frac{1}{T}\sum_{k=-\infty}^{\infty} X\left(\frac{\omega+2\pi k}{T}\right) \tag{7.108}$$

as desired. ■

Equation (7.108) shows that $S(\omega)$, the DTFT of $s(n)$, is the sum of an infinite number of copies of $Y(\omega)$, each translated by $2\pi k$ (Figure 7.16). Note that the sum of shifted copies of $Y(\omega)$ is 2π-periodic. The situation of interest is when there is no overlap in the shifted $Y(\omega)$ components in Figure 7.16. In this case, $Y(\omega)$ resembles a single period of the DTFT of $s(n)$, $S(\omega)$. We may recover $x(t)$ from the discrete samples, because we then know that $X(\omega) = TY(T\omega)$, and $x(t)$ derives from $X(\omega)$ via the FT synthesis equation. What criteria are necessary for there to be no overlap of the shifted versions of $Y(\omega)$? The famous Shannon–Nyquist theorem answers this question.

Theorem (Shannon–Nyquist Sampling Theorem). Suppose that $x(t) \in L^1$ is an analog signal, $T > 0$, and $s(n) = x(nT)$. If $s(n) \in l^1$, so that the DTFT sum converges uniformly to $S(\omega)$, then $x(t)$ may be recovered from the samples $s(n)$ if

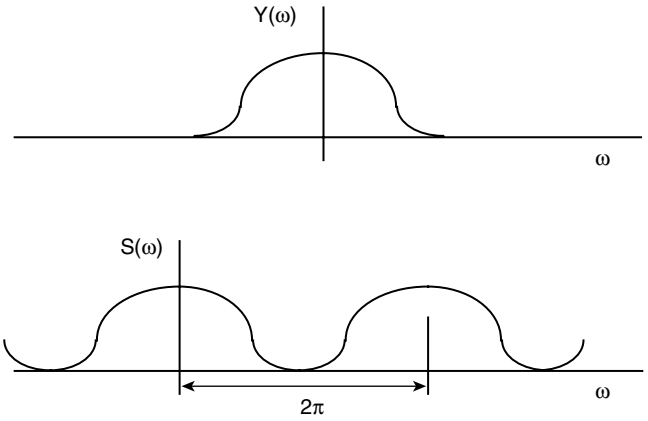

Fig. 7.16. S(ω) is the sum of shifted copies of $Y(\omega)$. If Y decays quickly in the frequency domain, then its translated copies overlap only slightly or not at all.

- $x(t)$ is band-limited.
- The sampling frequency $F = T^{-1} > 2F_{\max}$, where $|X(\omega)| = 0$ for $\omega > 2\pi F_{\max}$.

Proof: We deduce a series of equivalent criteria that prevent overlap. Now, since the difference between two translates is 2π, no overlap occurs when all of the nonzero values of $Y(\omega)$ lie within $[-\pi, \pi]$. Thus, $Y(\omega) = 0$ for $|\omega| > b > 0$, for some $b < \pi$. This means that $X(\omega) = 0$ for $|\omega| > |b/T|$, since $Y(\omega) = T^{-1}X(\omega/T)$. Equivalently, for no overlap, it must be the case that $x(t)$ is band-limited, and its nonzero spectral values within $[-\pi/T, \pi/T]$. Let $0 < B$ be the least upper bound of $\{\omega : X(\omega) > 0 \text{ or } X(-\omega) > 0\}$. Then $B < \pi/T$. But, B is measured in radians per second, and to give it in hertz we need to use the radians-to-hertz conversion formula, $\omega = 2\pi f$. Thus, the criterion for no overlap becomes $2\pi F_{\max} < \pi/T$, where $F_{\max}$ is the maximum frequency component of $x(t)$ in hertz, and T is the sampling period $s(n) = x(nT)$. Finally, this means precisely that $2F_{\max} < 1/T = F$. ■

When the analog signal $x(t)$ is not band-limited, aliasing is inevitable, because the shifted versions of $Y(\omega)$ must overlap. When $x(t)$ is band-limited and the sampling interval is too large, the shifted versions of $Y(\omega)$ overlap with one another and in their summation produce artifacts that are not part of the shape of the true analog spectrum of $x(t)$. Figure 7.17 illustrates a situation with aliasing.

These results motivate the following definition [3].

Definition (Nyquist Rate). If a signal $x(t)$ is band-limited, then its *Nyquist rate* is $F = 2F_{\max}$, where $F_{\max}$ is the least upper bound of values ω, where $|X(\omega)| \neq 0$.

Thus, sampling at intervals T such that $1/T$ is above the Nyquist rate permits perfect reconstruction of the analog signal $x(t)$ from its discrete samples, $s(n) = x(nT)$.

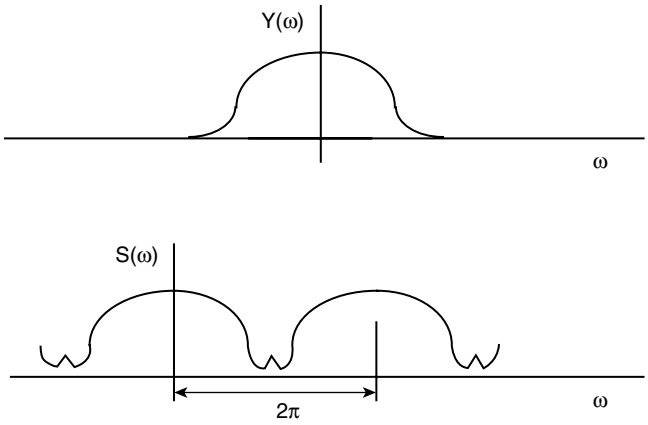

Fig. 7.17. Aliasing occurs when the shifted copies of $Y(\omega)$ overlap. In this situation, a single period of the spectrum of $s(n)$, $S(\omega)$, is *not* an exact replica of $X(\omega)$. High frequency components are added into some of the low frequency components. The result is that the reconstructed analog signal does not equal the original time domain signal, $x(t)$.

We now know, in principle, the conditions under which an analog signal may be reconstructed from its discrete samples. The next two sections limn out the theory of sampling. Section 7.3.3 provides an elegant reconstruction formula; it shows how to rebuild the analog signal from a simple set of interpolating signals. Section 7.3.4 casts a shadow on all these proceedings, however. A central result, the Uncertainty Principle, informs us that a signal with good frequency-domain behavior (as regards sampling and reconstruction) must have poor time-domain characteristics.

7.3.3 Reconstruction

The next theorem gives a formula for reconstructing, or interpolating, an analog signal from its samples. The conditions discovered above for ideal reconstruction must apply, of course. And there are some qualifications to this result that should be kept in mind:

- It assumes that perfect discrete samples are obtained in the sampling operation.
- The interpolating signals are not finitely supported.
- There are an infinite number of signals that must be summed to achieve perfect reconstruction.

Clearly, there are practical concerns with implementing analog signal reconstruction using this method. The reconstruction derives from evaluating the Fourier transform synthesis equation integral over a single period of the DTFT of $s(n)$, the signal samples.

Theorem (Shannon–Nyquist Interpolation Formula). Suppose that $x(t) \in L^1$ is an analog signal, $T > 0$, and $s(n) = x(nT)$. Let $s(n) \in l^1$ so that the DTFT sum converges uniformly to $S(\omega)$. Also, let $2F_{\max} < F = 1/T$, where $F_{\max}$ is the maximum frequency component of $x(t)$ in hertz. Then $x(t)$ may be recovered from $s(n)$ by the following sum:

$$x(t) = \sum_{n=-\infty}^{+\infty} s(n)\,\mathrm{sinc}\left(\frac{\pi t}{T} - n\pi\right) \tag{7.109}$$

Proof: The criterion for reconstruction applies, $x(t)$ is band-limited, and we find $x(t)$ from the IFT integral:

$$x(t) = \frac{1}{2\pi}\int_{-\infty}^{+\infty} X(\omega)\exp(j\omega t)\,d\omega = \frac{1}{2\pi}\int_{-\pi/T}^{+\pi/T} X(\omega)\exp(j\omega t)\,d\omega \tag{7.110}$$

Now, the DTFT of $s(n)$ is given by (7.108) for all $\omega \in \mathbb{R}$, and (because there is no overlap of the shifted versions of the Fourier transform) for $\omega \in [-\pi/T, \pi/T]$, we have $TS(\omega) = X(\omega/T)$, whence

$$x(t) = \frac{T}{2\pi}\int_{-\pi/T}^{+\pi/T} S(T\omega)\exp(j\omega t)\,d\omega \tag{7.111}$$

Inserting the DTFT analysis equation sum for $S(T\omega)$ in (7.111) and interchanging integration and summation gives

$$\begin{aligned} x(t) &= \frac{T}{2\pi}\int_{-\pi/T}^{+\pi/T}\left[\sum_{n=-\infty}^{\infty} s(n)\exp(-jT\omega n)\right]\exp(j\omega t)\,d\omega \\ &= \frac{T}{2\pi}\sum_{n=-\infty}^{\infty} s(n)\int_{-\pi/T}^{+\pi/T}\exp(-jT\omega n)\exp(j\omega t)\,d\omega \\ &= \frac{T}{2\pi}\sum_{n=-\infty}^{\infty} s(n)\int_{-\pi/T}^{+\pi/T}\exp[j\omega(t-Tn)]\,d\omega \end{aligned} \tag{7.112}$$

The last definite integral evaluates to a sinc signal:

$$\begin{aligned} x(t) &= \frac{T}{2\pi}\sum_{n=-\infty}^{\infty} s(n)\int_{-\pi/T}^{+\pi/T}\exp[j\omega(t-Tn)]\,d\omega = \sum_{n=-\infty}^{\infty} s(n)\frac{\sin\left[\frac{\pi}{T}(t-Tn)\right]}{\left[\frac{\pi}{T}(t-Tn)\right]} \\ &= \sum_{n=-\infty}^{\infty} s(n)\,\mathrm{sinc}\left(\frac{\pi t}{T} - \pi n\right) \end{aligned} \tag{7.113}$$

and the proof is complete. ■

Another way to interpret this result is to note that, for a given sampling interval T, the set of the analog sinc functions, $\text{sinc}(\pi t/T - \pi n)$, span the space of band-limited signals.

7.3.4 Uncertainty Principle

The concept of a band-limited signal demands further scrutiny. If it was not at the beginning of this discussion, it is certainly clear now how important band-limited signals are for signal processing. Whenever the motivation is to cast an analog signal in digital form and reproduce it—perhaps with some intermediate processing steps applied—then a major consideration is how well discrete samples can represent the original signal. Technologies such as compact disc players succeed or fail based on whether they can sample signals fast enough to beat the Nyquist rate. In analyzing a signal, we also begin with a real-world—analog—signal; then we sample it, process it, and load it into a computer. In the computer, software algorithms build a structural description of the signal and then attempt to classify, identify, and recognize the signal or its fragments. Admittedly, the algorithms may destroy the original form of the signal. But the representation by the interpolation formula is useful, since the coefficients of the expansion indicate a certain signal similarity to the interpolating sinc functions. These may be a basis for classification. And this whole classification procedure gets started with an observation that the source analog signals enjoy a strict limitation on the extent of their frequency content.

This does beg the question, How common are band-limited signals? A signal, $x(t)$, is band-limited when $X(\omega) = \mathcal{F}[x(t)]$ has finite support. If the signal is band-limited, but still has high-frequency components, then a proportionately higher sampling frequency is necessary for ideal signal reconstruction. So, in general, we seek signals whose spectral values are concentrated, or localized, about the origin, $\omega = 0$. We confess that real signals—be they analog or discrete—do not continue unabated forever in the time domain; they must eventually die out. And for practical reasons, such as available memory in a signal analysis system, this time-domain locality is an important consideration. But can we also expect good frequency-domain behavior from finitely supported analog signals?

It is easy to see that a nonzero signal cannot be finitely supported in both domains, because if $x(t)$ and $X(\omega)$ have finite support, then $x(t) = x(t)[u(t + a) - u(t - a)]$ for some $a > 0$. The FT of $x(t)$ is therefore the convolution of the FT of $x(t)$ and the analog boxcar signal $b(t) = u(t + a) - u(t - a)$. But $B(\omega)$ is a sinc-type function, and since $X(\omega)$ is nonzero, the convolution of the two in the frequency domain does not have finite support, a contradiction.

Let us state and prove another famous result, the Uncertainty Principle, which shows that there is an insurmountable tradeoff between frequency-domain locality and time-domain locality. First, however, we need to define the concept of the locality of a signal in the time and frequency domains. We invoke concepts from statistics; namely, the locality of a signal is associated with the second moment, or the variance, of its values.

Definition (Time- and Frequency-Domain Locality). The *time-domain locality* of a signal $x(t)$ is

$$\Delta_t^2(x) = \int_{-\infty}^{+\infty} |x(t)|^2 \, t^2 dt, \tag{7.114a}$$

and its *frequency-domain locality* is

$$\Delta_\omega^2(X) = \int_{-\infty}^{+\infty} |X(\omega)|^2 \, \omega^2 d\omega \tag{7.114b}$$

The uncertainty principle holds for signals that decay faster than the reciprocal square root signal. This is necessary for the convergence of the second-order moment integral.

Theorem (Uncertainty Principle). Suppose that $x(t)$ is an analog signal, $\|x\|_2 = 1$, and $x^2(t)t \to 0$ as $t \to \infty$. Then

$$\sqrt{\frac{\pi}{2}} \le \Delta_t(x)\Delta_\omega(X). \tag{7.115}$$

Proof: The idea is to apply the analog Cauchy–Schwarz inequality to $tx(t)x'(t)$:

$$\left| \int_{-\infty}^{+\infty} tx(t)x'(t)\, dt \right|^2 \le \int_{-\infty}^{+\infty} |tx(t)|^2 dt \int_{-\infty}^{+\infty} |x'(t)|^2 dt = \Delta_t^2(x) \int_{-\infty}^{+\infty} |x'(t)|^2 \tag{7.116}$$

Now, $x'(t)$ has radial FT $j\omega X(\omega)$, so the analog version of Parseval's formula (Chapter 5) implies that

$$\int_{-\infty}^{+\infty} |x'(t)|^2 = \frac{1}{2\pi}\Delta_\omega^2(X). \tag{7.117}$$

Hence,

$$\left| \int_{-\infty}^{+\infty} tx(t)x'(t)\, dt \right|^2 \le \Delta_t^2(x)\frac{1}{2\pi}\Delta_\omega^2(X). \tag{7.118}$$

The integral in (7.118) is our focus; using the chain rule on its integrand and then integrating it by parts gives

$$\int_{-\infty}^{+\infty} tx(t)x'(t)\,dt = \frac{1}{2}\int_{-\infty}^{+\infty} t\frac{\partial x^2(t)}{\partial t}x'(t)\,dt = \frac{1}{2}tx^2(t)\Big|_{-\infty}^{\infty} - \frac{1}{2}\int_{-\infty}^{+\infty} x^2(t)\,dt \tag{7.119}$$

Now, $x^2(t)t \to 0$ as $t \to \infty$ and $\|x\|_2 = 1$ imply

$$\int_{-\infty}^{+\infty} tx(t)x'(t)\,dt = \frac{1}{2}\int_{-\infty}^{+\infty} t\frac{\partial x^2(t)}{\partial t}x'(t)\,dt = 0 - \frac{1}{2}\int_{-\infty}^{+\infty} x^2(t)\,dt = -\frac{1}{2}\|x\|^2 = -\frac{1}{2}. \tag{7.120}$$

Hence, from (7.118),

$$\left|-\frac{1}{2}\right|^2 = \frac{1}{4} \le \Delta_t^2(x)\frac{1}{2\pi}\Delta_\omega^2(X), \tag{7.121}$$

from which (7.115) follows. ■

In the exercises, it is shown that the Gaussian signal achieves this lower bound in the product of joint time- and frequency- domain locality.

Thinking about the Fourier transform and the Uncertainty Principle, we can understand how poor is its joint locality. Allowing that we may Fourier transform signals of slow decay (Chapter 6) using the generalized FT, the FT of a sinusoid is a pair of pulses in the frequency domain. Also, the FT of a pulse $\delta(t)$ is the constant $\omega = 1$. Thus, signals with extreme locality in one domain transform into signals with no locality whatsoever in the other domain. We will discover the problems that this lack of joint locality causes when we work through frequency-domain applications in Chapter 9. Chapters 10 and 11 develop transformation theories—very modern theories, it turns out—that furnish good local time and frequency decompositions of signals. Finally, in the last chapter, we apply these short-time Fourier and wavelet transforms to signal analysis problems.

7.4 SUMMARY

The detailed investigation and intense interest in discrete frequency transforms is a relatively recent phenomenon, and this is an altogether curious circumstance in view of the very tractable nature of the mathematical underpinnings. Analog theory—as some readers now just catching their breath would doubtlessly urge—is much more difficult. Historically, discrete frequency transforms have been explored since the time of Gauss, but it is only with the development of digital computers that the fast computational methods have attracted wide interest and investigation.

Most of the exercises are basic problems that reinforce the concepts developed in the text. The next chapter considers an extension of the DTFT, called the z-transform. Chapter 9 considers applications of frequency-domain analysis to signal interpretation problems.

REFERENCES

1. J. W. Cooley and J. W. Tukey, An algorithm for the machine calculation of complex Fourier series, *Mathematics of Computation,* vol. 19, pp. 297–301, 1965.
2. C. E. Shannon, A mathematical theory of communication, *Bell Systems Technical Journal,* vol. 27, pp. 379–423 and pp. 623–656, 1948.
3. H. Nyquist, Certain topics in telegraph transmission theory, *Transactions of the AIEE,* vol. 47, pp. 617-644, 1928.
4. J. W. Cooley, P. A. Lewis, and P. D. Welch, Historical notes on the fast Fourier transform, *IEEE Transactions on Audio and Electroacoustics,* vol. AU-15, pp. 76–79, June 1967.
5. P. J. Plauger, *The C++ Standard Library*, PTR Publishers, 1997.
6. DSP Committee of the IEEE Society for Acoustics, Speech, and Signal Processing, *Programs for Digital Signal Processing*, New York: IEEE Press, 1979.
7. W. H. Press, B. P. Flannery, S. A. Teukolsky, and W. T. Vetterling, *Numerical Recipes*, Cambridge: Cambridge University Press, 1986.
8. C. S. Burrus and T. W. Parks, *DFT/FFT and Convolution Algorithms: Theory and Implementation*, New York: Wiley, 1985.
9. S. D. Stearns and R. A. David, *Signal Processing Algorithms in FORTRAN and C*, Englewood Cliffs, NJ: Prentice-Hall, 1988.
10. W. H. Press, B. P. Flannery, S. A. Teukolsky, and W. T. Vetterling, *Numerical Recipes in C*, Cambridge: Cambridge University Press, 1988.
11. H. S. Stone, *High-Performance Computer Architecture*, Reading, MA: Addison-Wesley, 1987.
12. *DSP56000/56001 Digital Signal Processor User's Manual*, Motorola, Inc., 1990.
13. M. Rosenlicht, *Introduction to Analysis*, New York: Dover, 1986.
14. E. Hille, *Analytic Function Theory*, vol. I, Waltham, MA: Blaisdell, 1959.
15. H. S. Carslaw, *An Introduction to the Theory of Fourier's Series and Integrals*, 3rd ed., New York: Dover, 1950.
16. H. F. Davis, *Fourier Series and Orthogonal Functions*, New York: Dover, 1963.
17. J. S. Walker, *Fourier Analysis*, New York: Oxford University Press, 1988.
18. D. C. Champeney, *A Handbook of Fourier Theorems*, Cambridge: Cambridge University Press, 1987.
19. L. Carleson, On convergence and growth of partial sums of Fourier series, *Acta Mathematica,* vol. 116, pp. 135–157, 1966.
20. R. A. Hunt, in *Orthogonal Expansions and Their Continuous Analogues*, Carbondale, IL: Southern Illinois University Press, pp. 235–255, 1968.
21. A. Zygmund, *Trigonometric Series*, vols. 1–2, Cambridge: Cambridge University Press, 1959.
22. Y. Katznelson, *An Introduction to Harmonic Analysis,* New York: Dover, 1976.

PROBLEMS

1. 1.For each of the following signals, $x(n)$, and intervals, $[0, N-1]$, find the discrete Fourier transform (DFT), $X(k)$:

(a) $x(n) = \cos(\pi n/3)$ on $[0, 5]$

(b) $x(n) = \sin(\pi n/3)$ on $[0, 5]$

(c) $x(n) = \cos(\pi n/3)$ on $[0, 11]$

(d) $x(n) = 3\sin(\pi n/3) + \cos(4\pi n/3)$ on $[0, 11]$

(e) $x(n) = \exp(4\pi n/5)$ on $[0, 9]$

(f) $x(n) = \cos(2\pi n/5 + \pi/4)$ on $[0, 4]$

2. Let $X = \mathcal{F}x$ be the system that accepts a signal of period $N > 0$ at its input and outputs the DFT of x.

(a) Show that the system $\mathcal{F}$ is linear. That is, suppose that discrete signals $x(n)$ and $y(n)$ both have period $N > 0$. Show that the DFT of $s(n) = x(n) + y(n)$ is $S(k) = X(k) + Y(k)$, where $X(k)$ and $Y(k)$ are the DFTs of $x(n)$ and $y(n)$, respectively.

(b) Show that the system $\mathcal{F}$ is not translation-invariant.

3. We may apply either the DFT or IDFT equation to transform a signal $x(n)$. Suppose that $x(n)$ has period $N > 0$.

(a) Show that the DFT and the IDFT of $x(n)$ both have period N.

(b) Show that if $X(k)$ is the DFT of $x(n)$, then the DFT of $X(k)$ is $Nx(-k)$.

4. Suppose the discrete signal, $x(n)$, has support on the finite interval, $[0, N-1]$, where $N > 0$.

(a) Show that the signal $x_p(n)$ defined by

$$x_p(n) = \sum_{k=-\infty}^{\infty} x(n - kN) \tag{7.122}$$

is periodic with period N and is identical to $x(n)$ on $[0, N-1]$.

(b) Suppose we perform the DFT analysis equation calculation for $x(n)$'s values on $[0, N-1]$, giving $X(0)$, $X(1)$, ... , $X(N-1)$. Then define $y(n) = (1/N)[X(0) + X(1)e^{2\pi jkn/N} + \cdots + X(N-1)e^{2\pi j(N-1)n/N}$. Show that $y(n) = x_p(n)$ for all n.

5. Some of the first examples in this chapter showed that the delta signal $\delta(n)$ has DFT $\Delta(k) = 1$, and the signal signal $x(n) = [\underline{1}, 1, 1, 1, 0, 0, 0, 0]$ has DFT $X(k) = [\underline{4}, 1 - (1 + \sqrt{2})j, 0, 1 - (\sqrt{2} - 1)j, 0, 1 + (\sqrt{2} - 1)j, 0, 1 + (1 + \sqrt{2})j]$ on the interval $[0, 7]$. Find the DFT of the following signals, using only the properties of the DFT and without explicitly computing the DFT analysis equation's summation of products.

(a) $y(n) = x(n-1) = [\underline{0}, 1, 1, 1, 1, 0, 0, 0]$

(b) $y(n-k)$ for some $0 < k < 8$

(c) $y(n) = x(n) + \delta(n) = [\underline{2}, 1, 1, 1, 0, 0, 0, 0]$

(d) $y(n) = x(n) + \delta(n-3)$

6. Prove the Convolution in Frequency Theorem. That is, let $x(n)$ and $y(n)$ be periodic signals with period $N > 0$; let $X(k)$ and $Y(k)$ be their DFTs; and let $z(n) = x(n)y(n)$, the termwise product of x and y. Show that the DFT of $z(n)$ is $Z(k) = (1/N)X(k)*Y(k)$, where $X(k)*Y(k)$ is the discrete convolution of $X(k)$ and $Y(k)$.

7. Let signal $x(n)$ be real-valued with period $N > 0$, and let $X(k)$ be its DFT. Prove the following symmetry properties:

(a) $\mathrm{Re}[X(k)] = \mathrm{Re}[X^*(N-k)] = \mathrm{Re}[X^*(-k)]$

(b) $\mathrm{Im}[X(k)] = -\mathrm{Im}[X^*(N-k)]$

(c) $|X(k)| = |X(N-k)|$

(d) $\arg(X(k)) = -\arg(X(n-k))$.

8. Suppose the DTFT, $X(\omega)$, of the signal $x(n)$ exists. Show that $X(\omega)$ is periodic with period 2π.

9. Suppose that H is a linear, translation-invariant (LTI) system, and let $h(n)$ be its impulse response.

(a) Suppose H is a finite impulse response (FIR) system. Show that the DTFT of $h(n)$, $H(\omega)$, exists.

(b) Suppose H is stable: if $x(n)$ is bounded, then $y = Hx$ is also bounded. Show that $H(\omega)$ exists.

10. Consider the two Hilbert spaces, l^2 and $L^2[a, b]$, where $a < b$. (Consider two signals in $L^2[a, b]$ to be the same if they are equal except on a set of Lebesgue measure zero.)

(a) Show that there is an isomorphism between the discrete Hilbert space l^2 and the analog Hilbert space $L^2[a, b]$.

(b) Give an explicit definition of a mapping, $\mathcal{G}$, between them that effects the isomorphism.

(c) The shifted impulses $\{u(n-k): k \in \mathbb{Z}\}$ constitute an orthogonal basis set for l^2; find, therefore, their image under G and show that it is an orthogonal basis as well.

(d) Are the exponential signals $\{\exp(j\omega n): k \in \mathbb{Z}\}$ an orthogonal basis set for $L^2[a, b]$? Explain.

11. Derive the following properties of the Dirichlet kernel, $D_N(\theta)$.

(a) Use the properties of the exponential function $\exp(j\theta n)$ to show

$$D_N(\theta) = \frac{1}{2\pi}\sum_{n=-N}^{n=+N} \exp(j\theta n) = \frac{1}{2\pi} + \frac{1}{\pi}\sum_{n=1}^{n=N} \cos(\theta n).$$

(b) Use the closed-form expression for the partial geometric series summation to show

$$D_N(\theta) = \frac{1}{2\pi} \frac{\sin\left(N\theta + \frac{\theta}{2}\right)}{\sin\left(\frac{\theta}{2}\right)}.$$

(c) Use (a) to prove

$$\int_0^{\pi} D_N(\theta)\, d\theta = \frac{1}{2} = \int_{-\pi}^{0} D_N(\theta)\, d\theta.$$

(d) From (b), show that $D_N(\theta)$ has its first two zero crossings at the points $\theta_N = \pm\pi/(N + 1/2)$. What is $D_N(0)$?

(e) Use (b) to sketch $D_N(\theta)$ for various values of N. Explain how $D_N(\theta)$ may be considered as the high-frequency sinusoid $\sin(N\theta + \theta/2)$ bounded above by the cosecant envelope $[\csc(\theta/2)]/(2\pi)$ and below by $-[\csc(\theta/2)]/(2\pi)$.

12. Consider the mapping $\mathcal{F}$ that takes $x(n) \in l^2$ to $X(\omega) \in L^2[-\pi, \pi]$, where $X(\omega)$ is the DTFT of $x(n)$. Show that $\mathcal{F}$ is linear, but not quite an isomorphism. Explain how to modify $\mathcal{F}$ so that it becomes a Hilbert space isomorphism.

13. Find the DTFT of the following signals.

(a) $e_k(n) = \delta(n - k)$

(b) $b(n) = [1, 1, 1, \underline{1}, 1, 1, 1]$

(c) $a(n) = b(n) + e_2(n) + 4e_{-3}(n)$

(d) $s(n) = (1/3)^n u(n)$

(e) $x(n) = (5)^n u(2 - n)$

(f) $h(n) = s(n) + 4b(n)$

(g) $y(n) = (x * h)(n)$

14. Find the IDTFT of the following signals.

(a) $E_k(\omega) = \exp(j\omega k)$

(b) $S(\omega) = 3\sin(-7j\omega)$

(c) $C(\omega) = 2\cos(3j\omega)$

(d) $P(\omega) = S(\omega)C(\omega)$

15. Let $x(n)$ and $y(n)$ be discrete signals and $X(\omega)$ and $Y(\omega)$ be their respective DTFTs. Then show the following linearity, time shift, frequency shift, and time reverse properties:

(a) The DTFT of $ax(n) + by(n)$ is $aX(\omega) + bY(\omega)$.

(b) The DTFT of $x(n - m)$ is $\exp(-j\omega m)X(\omega)$.

(c) The IDTFT of $X(\omega - \theta)$ is $\exp(-j\theta n)x(n)$.

(d) The DTFT of $x(-n)$ is $X(-\omega)$.

16. Let the signal $x(n)$ be real-valued and let $X(\omega)$ be its DTFT. If $z \in \mathbb{C}$, then let z^* be the complex conjugate of z, let Real(z) be its real part, let Imag(z) be its imaginary part, and let $\arg(z) = \tan^{-1}[\text{Imag}(z)/\text{Real}(z)]$ be the argument of z. Prove the following symmetry properties:

(a) $\text{Real}(X(\omega)) = \text{Real}(X(-\omega))$

(b) $-\text{Imag}(X(\omega)) = \text{Imag}(X(-\omega))$

(c) $X(\omega) = X^*(-\omega)$

(d) $|X(\omega)| = |X(-\omega)|$

(e) $\arg(X(\omega)) = -\arg(X(-\omega))$

17. Let the signal $x(n)$ be real-valued and $X(\omega)$ be its DTFT. If $x_e(n) = [x(n) + x(-n)]/2$ is the even part of $x(n)$, and $x_o(n) = [x(n) - x(-n)]/2$ is the odd part of $x(n)$, then find

(a) The DTFT of $x_e(n)$

(b) The DTFT of $x_o(n)$

18. Let the signal $x(n)$ be real-valued and let $X(\omega)$ be its DTFT. Show the following symmetry properties, which use the notation of the previous two problems:

(a) The DTFT of $x^*(n)$ is $X^*(-\omega)$, and the DTFT of $x^*(-n)$ is $X^*(\omega)$.

(b) The DTFT of $x_e(n)$ is $\text{Real}(X(\omega))$, and the DTFT of $x_o(n)$ is $j[\text{Imag}(X(\omega))]$.

(c) The DTFT of $\text{Real}(X(n))$ is $X_e(\omega)$, and the DTFT of $j[\text{Imag}(X(n))]$ is $X_o(\omega)$.

19. We know that the perfect high-frequency removal (low-pass) filter has impulse response

$$h(n) = \frac{\omega_c}{\pi}\text{sinc}(n\omega_c) = \frac{\omega_c}{\pi}\frac{\sin(n\omega_c)}{n\omega_c} = \frac{\sin(n\omega_c)}{n\pi}.$$

(a) Consider the discrete system whose frequency response, $G(\omega)$, is unity for $|\omega| > \omega_c$ and zero otherwise. Explain why G may be considered a perfect high-pass filter. Find the time-domain filter, $g(n)$, corresponding to $G(\omega)$. Is $g(n)$ physically implementable? Explain.

(b) Consider the discrete system whose frequency response, $P(\omega)$, is unity for $\omega_h \geq |\omega| \geq \omega_l$ and zero otherwise. Explain the description of P as being an ideal bandpass filter. Find the time-domain filter, $g(n)$, corresponding to $G(\omega)$. Is $g(n)$ physically implementable? Explain.

(c) If $h(n)$ is an ideal time-domain low-pass filter, it is possible to approximate it by a finitely supported filter by zeroing terms above $n = N > 0$. In signal analysis applications, such as Chapter 4 considered, explain the possible uses of such a filter. For what types of applications is this filter useful? What applications are not served by this filter?

(d) Consider the questions in part (c) for perfect high-pass and bandpass filters.

20. Analog signal $x(t)$ has radial FT $X(\omega)$ shown below.

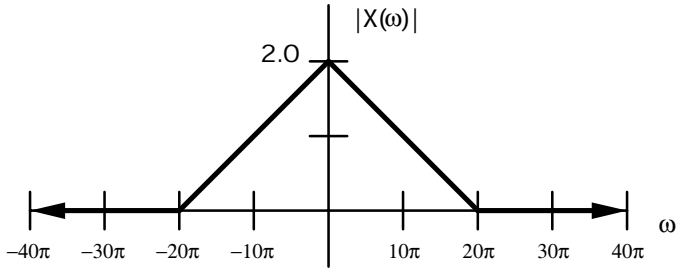

(a) What is the Nyquist rate for this signal in hertz?

(b) If $s(n) = x(nT)$, where $1/T = F = 15$ hertz, sketch the DTFT of s, $S(\omega)$.

(c) Sketch the radial FT of an ideal low-pass filter H such $y = Hs$ is not aliased when sampled at $F_S = 15$ hertz.

The remaining problems extend some of the ideas in the text.

21. Suppose we are given a formula for the DTFT of a discrete signal $h(n)$: $H(\omega) = P(\omega)/Q(\omega)$, where P and Q are both polynomials in ω. Develop two methods to find $h(n)$.

22. Show that a nonzero signal $x(n)$ cannot be finitely supported in both the time and frequency domains.

(a) Show that there is a $k > 0$ such that $x(n) = x(n)[u(n + k) - u(n - k)] = x(n)b(n)$, where $u(n)$ is the discrete unit step signal.

(b) Find the discrete-time Fourier transform of $b(n)$: $B(\omega)$.

(c) Apply the Convolution-in-Frequency Theorem to the product $x(n)b(n)$ to find an equivalent expression for $X(\omega)$.

(d) Derive a contradiction from the two expressions for $X(\omega)$.

23. Let $g(t) = A\exp(-\sigma t^2)$. Use the conditions for equality in the analog Schwarz inequality, and find constants A and σ so that

$$\sqrt{\frac{\pi}{2}} \leq \Delta_t\,(g)\Delta_\omega(G)$$